

Data Report on Mapping the Hydrogeology of the Clarkson Area within the Lower Elkhorn Natural Resources District Using an Airborne Electromagnetic Survey

Jared D. Abraham
Clint P. Carney P.G.
James C. Cannia P.G.

Prepared for the Lower Elkhorn Natural Resources District





December 30, 2013

Data Report on Mapping the Hydrogeology of the Clarkson Area within the Lower Elkhorn Natural Resources District Using an Airborne Electromagnetic Survey

Prepared for:

The Lower Elkhorn Natural Resources District
601 E Benjamin Ave
Norfolk, NE 68701

Submitted by:

Exploration Resources International Geophysics, LLC
6207 Hwy 80 East
Vicksburg, MS 39180
Phone: (866) 974-6867

Jared D. Abraham

Jared.Abraham@xrigeo.com

Clint P. Carney P.G.

Clint.Carney@xrigeo.com

James C. Cannia, P.G.

Jim.Cannia@xrigeo.com



Table of Contents

Executive Summary.....	1
Introduction	2
Purpose and Scope	2
Description of the Project Area	2
Airborne Electromagnetic Survey.....	3
Method.....	3
AEM Measurements	5
AEM Data Processing	5
Automatic Processing.....	5
Manual Processing and Laterally Constrained Inversions.....	7
Spatially Constrained Inversion.....	7
Data display and interpretation.....	7
Hydrogeology of the Project Area	8
Physical Setting	8
Surface Hydrology	8
Geologic Setting.....	8
Quaternary Geology	8
Hydrogeology of Quaternary Deposits.....	9
Cretaceous Geology and Aquifer Potential.....	12
Interpretation of AEM Results	12
Map of the Principal Aquifer.....	12
Estimate of Aquifer Volume	14
Relationship to Current Test Holes and Extraction Wells.....	14
Estimated Potential Recharge Areas	16
Bedrock Aquifer Potential.....	17
Summary and Recommendations	18
Bibliography	19
Appendix 1 AEM Interpretive Imagery.....	24
Appendix 2- Metadata	45
Appendix 3- Ancillary Data	49

List of Figures

Figure 1 – Project Area location.	3
Figure 2 – Flight line locations over the Project Area.....	6
Figure 3 – Locations of registered wells by use and CSD test holes in the Project Area.	10
Figure 4 – Observed water levels at five locations provided by the Lower Elkhorn NRD for the 2008-2013 time period.....	11

Figure 5 – Comparison of the subsurface resistivity and lithologic classifications.....15

Figure 6 - Comparison of the resistivity values from testhole 16 inch normal log of 02-LE-13 (blue line) and an inverted forward modeled response from that log using the SkyTEM 304 system characteristics and inversion settings.....16

NOTE: A list of figures in Appendix 1 is provided at the beginning of the appendix.

Length and Flow Rate Conversion Factors

Multiply	By	To Obtain
	Length	
kilometers	0.62	miles
meters	3.28	feet
millimeters	0.039	inches
	Flow Rate	
cubic meters/minute	264.2	gallons/minute
cubic meters/minute	0.59	cubic feet/second

Executive Summary

Exploration Resources International (XRI) is pleased to submit our report to the Lower Elkhorn Natural Resources District (LENRD) titled "Mapping the Hydrogeology of the Clarkson Area within the Lower Elkhorn Natural Resources District Using Airborne Electromagnetic Survey." This project began in August 2013 to address the water resource concerns of the LENRD in the area between the towns of Clarkson and Howells. This area experienced record groundwater declines during 2012 that caused the LENRD to look for additional information on the groundwater of the area. XRI entered into an agreement with LENRD to undertake a hydrogeologic study of the area.

The scope of work for this project was as follows:

An Airborne Electromagnetic (AEM) survey will be flown over a specified area near the town of Clarkson, Nebraska within the LENRD to support creation of the hydrogeological framework of this area. This framework will be provided as preliminary AEM data and as a final product in a data report. The AEM survey will be flown at approximately 300 meter spacing in an east-west direction and approximately 1500 meter spacing in a north-south direction. Approximately 400 kilometers of AEM survey will be flown.

- A. The Contractor shall acquire an AEM survey flown over the LENRD to provide the hydrogeological framework, commencing on approximately August 1, 2013. Status reports of the flying will be provided to the LENRD daily, including the areas flown, production rates, and flight plan for the following day.
- B. The Contractor shall process and quality assure/quality control all of the data collected from the AEM and ground system.
- C. The Contractor shall invert the AEM data and then derive a 3D electrical model of the surveyed area. These inverted, georeferenced data will be delivered to the LENRD.
- D. The Contractor shall provide a hydrogeologic framework report that will include maps of aquifer(s), estimate of aquifer(s) volume, map of aquifer(s) relationship to current test holes and production groundwater wells, and a map of estimated potential recharge areas. The report will also include all data and metadata files. The report will be delivered in PDF digital format.

Introduction

Purpose and Scope

Water management in eastern Nebraska has increased the need for detailed hydrogeologic frameworks for selected areas of the LENRD. Water management in the Elkhorn River basin continues to be a difficult task for water managers and users alike. Recent drought conditions (2012) in the LENRD have shown that the project area between the towns of Clarkson and Howells have severe water supply problems that cannot be understood with current hydrogeologic information. For the LENRD to effectively utilize their groundwater management plan, they need detailed information on the aquifers in the area. In particular, they need to understand the aquifer characteristics, interconnection with surface water, interconnection with adjacent aquifers and connection to the existing groundwater production wells. There are six (6) Conservation and Survey Division (CSD) test holes in or near the project area. These test holes are vital to the understanding of the area, but they cannot provide enough information to complete a detailed hydrogeologic framework.

Selection of the appropriate management activities is vital to securing a viable water supply for this area and implementation of these activities can be expensive and time consuming to design and implement. They are often challenged by other interests as to their effectiveness and suitability to provide equitable water use within the basin; therefore, it is recommended that AEM surveys be performed to supplement the testhole information and be used to develop a new hydrogeologic framework of the project area. Historical AEM work in the Oakland area of eastern Nebraska has indicated that Time Domain AEM is the most suitable for mapping glacial aquifers within the thick till sequence of eastern Nebraska (Abraham and others, 2011a). Detailed hydrogeologic frameworks will give greater confidence to regulators, investors, and the public in water management decisions and practices because the understanding of the natural system is represented in detail never before achieved. This information also allows for future exploration of undeveloped potential groundwater resources.

Traditional geologic information must be part of any AEM study, and it will be included in the hydrogeologic framework generated for this project. The hydrogeologic frameworks developed from the AEM data allow the user to visualize the subsurface in three dimensions. A three-dimensional evaluation of the aquifer can be made to estimate various percentages of the aquifer materials and their location/relationship to existing extraction wells.

The AEM survey provides nearly continuous data of the subsurface. It is acquired quickly without trespass onto private property. Once acquired, it can then be analyzed quickly and related to materials composing the aquifer.

Description of the Project Area

The project area overlies the boundary junction of Colfax, Cuming, and Stanton Counties and is approximately one township in area. The towns of Clarkson and Howells lie on the west and east end of the project area, respectively (Figure 1). This area is glaciated and the

topography and landforms of the area reflect this. A series of moraines oriented approximately north-south make up the rolling hills between the valleys. The hydrogeology of the area is defined by this glacial history and will be discussed later in the report. Agriculture is the main economic activity of the area. Groundwater supply is limited to the coarse glacial sediment packages that occupy a small percentage of the project area.

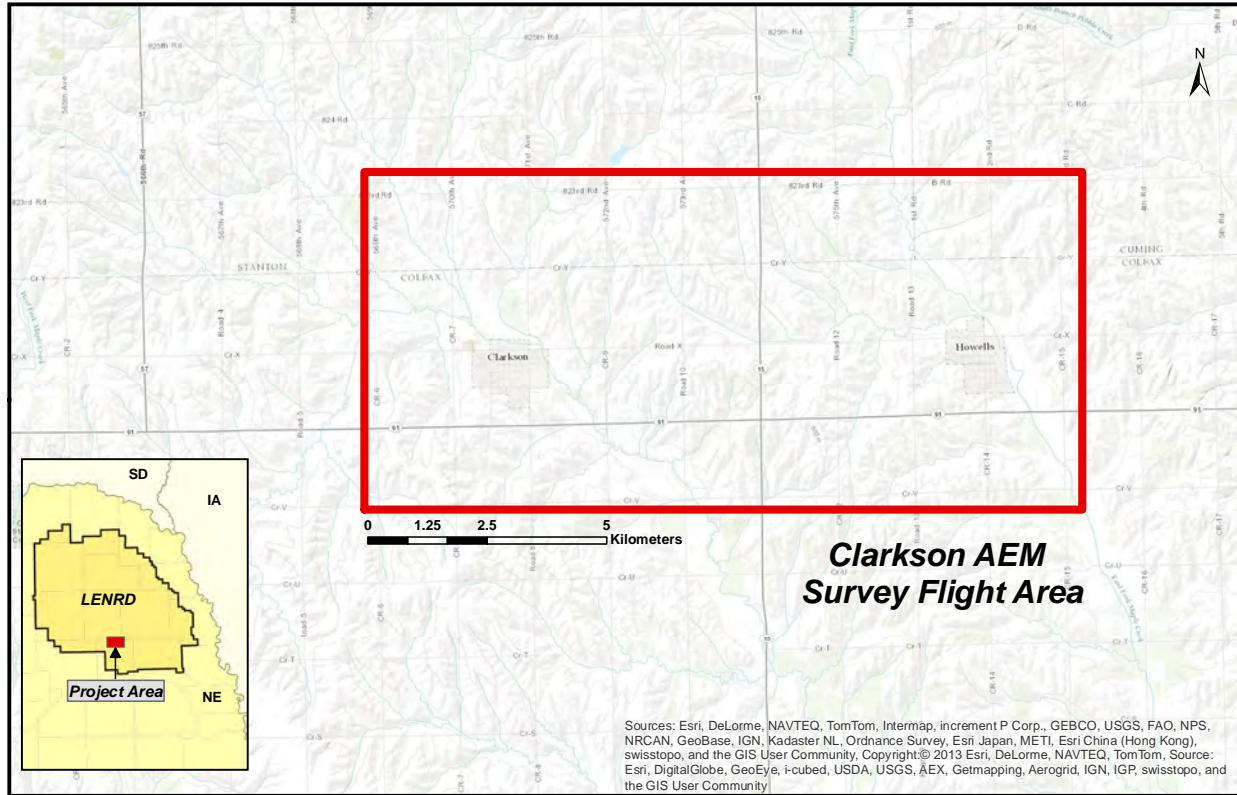


Figure 1 – Project Area location.

Airborne Electromagnetic Survey

Method

Airborne electromagnetic (AEM) surveys, flown with either helicopter or fixed-wing aircraft, increasingly have been employed to characterize aquifers and their geologic setting (Fitterman and Deszcz-Pan, 1998; Wynn, 2002; Jørgensen and others, 2003; Paine and Minty, 2005; Møller and others, 2009; Viezzoli and others, 2010; Abraham and others, 2011a, Abraham and others, 2011b., Jorgensen and others, 2012; Oldenborger and others, 2013, Lawrie and others, 2013). Such AEM surveys can provide characterization of electrical properties of earth materials from the near-surface 1 to 3 meters down to depths of 300 to 600 m. Typical AEM systems transmit an electromagnetic (radio-frequency) signal that interacts with the earth to generate (induce) secondary currents. Those secondary currents are a function of the subsurface electrical resistivity, which is controlled by the amount of mineralogical clay, gravel, water content (and the dissolved solids in the water), metallic mineralization, and void space. Measurements of the secondary currents are recorded either in the time domain (where the signal is a train of pulses and

measurements are taken between the primary field pulses as a function of time as the secondary currents decay) or in the frequency domain (where the signal is a continuous wave and measurements are taken at the frequency of the primary field, which is still present). Using numerical imaging and inversion, depth sections of estimated electrical resistivity can be created along flight lines. Interpolations between flight lines provide an estimation of the 3D distribution of electrical resistivity and is represented as a 3-D resistivity model.

Obtaining a reliable AEM-derived resistivity model requires complete system characterization including 1) geometry; 2) frequencies and bandwidth; 3) transmitter waveform characteristics; 4) timing; 5) and 6) accurate modeling (Christiansen and others, 2011). Poor AEM modeling assumptions can lead to errors in the resulting resistivity models and, in turn, the hydrologic and geologic interpretations (Viezzoli and others, 2013). These effects can include erroneous resistive or conductive layers and skewed estimates depth to interfaces. Inverting AEM data with an incomplete system description will commonly lead to a realistic, but incorrect earth resistivity model that fits the data to within measured or estimated data errors.

Electromagnetic geophysical methods detect variations in the electrical properties of rocks ρ in particular, electrical resistivity, or its inverse, electrical conductivity. Electrical resistivity can be correlated with geologic units on the surface and at depth using lithologic logs to provide a 3-D picture of subsurface geology. In the upper crust, the resistivities of geologic units are largely dependent upon their fluid content, pore-volume porosity, effective porosity, and conductive mineral content (Keller, 1989). While there is not a one-to-one relationship between lithology and resistivity, there are general correlations that can be made using typical values, even though values can be found at other localities that may fall outside of the ranges presented herein (Palacky, 1987). Fluids within the pore spaces and fracture openings can reduce electrical resistivities in what would otherwise be a resistive rock matrix, especially if the fluids are high in total-dissolved solids.

Resistivity can also be lowered by the presence of electrically conductive clay minerals, graphitic carbon, and metallic mineralization. For example, it is common for altered volcanic rocks to contain replacement minerals that have resistivities 10 times lower than those of the surrounding rocks (Nelson and Anderson, 1992). Fine-grained sediments, such as clay-rich alluvium, marine shales, and other mudstones, are normally conductive from a few ohm-m to a few tens of ohm-m (Keller, 1987; Palacky, 1987). Metamorphic rocks (nongraphitic) and unaltered, unfractured igneous rocks are normally moderately to highly resistive (a few hundreds to thousands of ohm-m). Carbonate rocks can have similarly high resistivities depending on their fluid content, porosity, and impurities (Keller, 1987; Palacky, 1987). Fault zones may be moderately conductive (tens of ohm-m) when composed of rocks fractured enough to have hosted fluid transport and consequent mineralogical alteration (Eberhart-Phillips and others, 1995). Higher subsurface temperatures cause higher ionic mobility that reduces rock resistivities (Keller, 1987; Palacky, 1987). Tables of electrical resistivity for a variety of rocks, minerals, and geological environments are in Keller (1987) and Palacky (1987).

AEM Measurements

The AEM measurements were completed with the SkyTEM 304 system. The SkyTEM system is a rigid frame, dual-moment Transient Electromagnetic (TEM) system developed over the past ten years (Sørensen and Auken, 2004). In contrast to the other TEM systems, the SkyTEM system has the receiver coil positioned slightly behind the transmitter wire in a null position, where the intensity of the primary field is minimized. The SkyTEM system was initially designed for groundwater mapping, and to this end employs two transmitter moments with different currents and different numbers of transmitter wire turns. The low current, or low moment (LM) mode, with a moment of 3,140 NIA, is used to record early-time gates which constrain near-surface information, while the high current, or high moment (HM) mode, with a moment of 145,000 NIA, improves the signal-to-noise ratio at late time gates.

The SkyTEM system flown for this study, SkyTEM 304, has a transmitter area of 314 m², and is intermediate between the SkyTEM 101 system, used for near-surface applications, and the SkyTEM 508, designed for deeper investigations. The SkyTEM 304 system records time gates from 1.6 μ s to 11 ms. The gates interpreted in the Clarkson survey fall between 9.6 μ s and 7.0 ms, with the latest recorded gates being too noisy to be used, and the gates before 5 μ s contaminated by residual primary field.

The SkyTEM system is calibrated to a ground test site in Lyngby, Denmark (HGG, 2010; HGG, 2011; Foged and others, 2013). Approximately, 400 line km were flown within the Clarkson, Nebraska area (Figure 2). Flight operations began on August 9 and continued through August 11, 2013.

AEM Data Processing

The Aarhus Geophysics Workbench version 4.1.1.765 (Aarhus Geophysics, 2013) was used for the processing and inversion of the AEM data. The Aarhus Geophysics Workbench was developed by the Hydrogeophysics Group at the University of Aarhus in Aarhus, Denmark (Auken and Christiansen, 2004; Viezzoli and others, 2008; Auken and others, 2009; Christiansen and Auken, 2012; Aarhus Geophysics, 2013). The Workbench is a complete processing and inversions tool and can be used with many types of AEM data. The Workbench is specifically well suited for editing AEM data and removing couplings to power lines and pipelines.

Automatic Processing

The AEM data were first run through automatic processing algorithms within Workbench. The GPS locations were filtered using a stepwise second order polynomial filter of 9 seconds, with a step length of 0.5 seconds. Filters were also applied to both of the tilt meter readings, a median filter of 3 seconds and an average filter of 2 seconds. The AEM data are corrected for tilt deviations from level. The altitude data are corrected using a series of two polynomial filters. The length of both eighth-order polynomial filters were set to 30

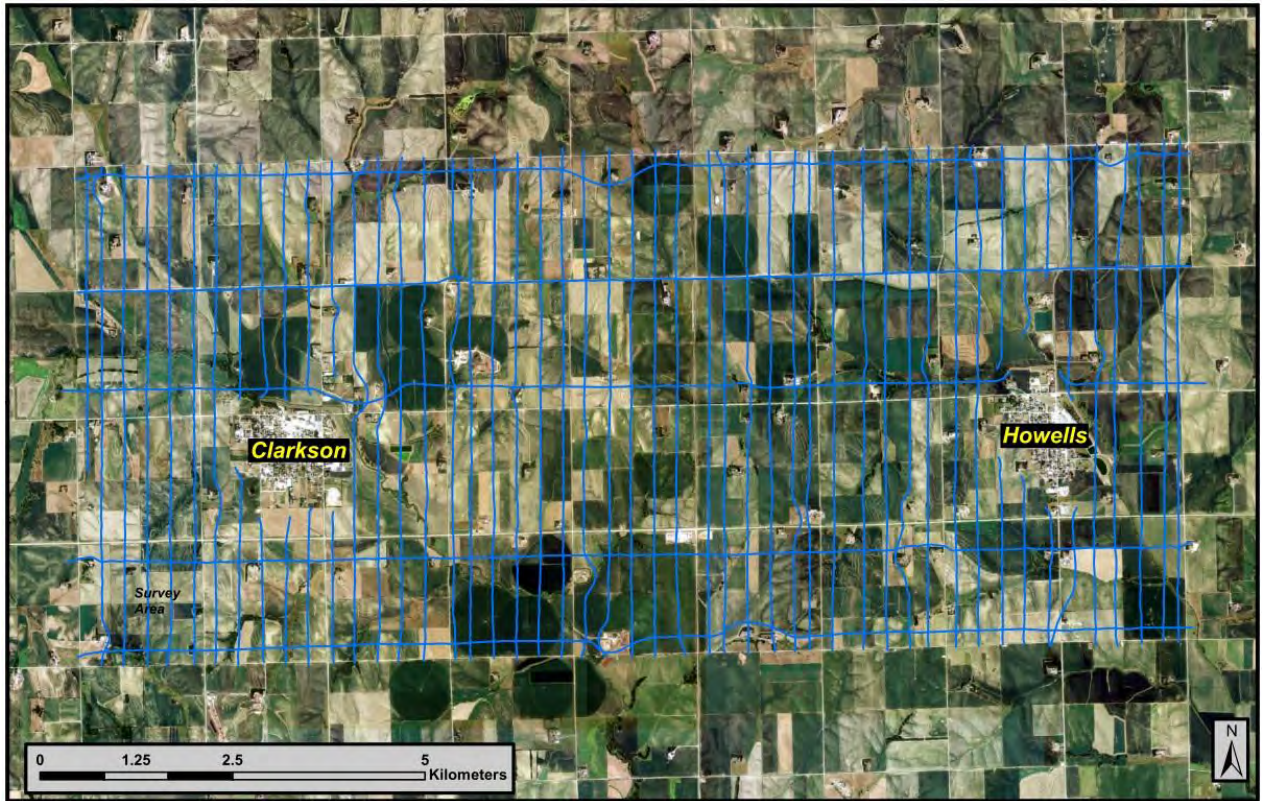


Figure 2 – Flight line locations over the Project Area.

seconds with shifts length of 6 seconds. The lower and upper thresholds were 1 and 30 meters, respectively.

The AEM data are run through several different filters including slope, sign, and trapezoidal filters. The cap sign filters culls data when the value changes sign and began at $1.5e^{-5}$ seconds for the low moment and $1e^{-4}$ seconds for the high moment. The noise level for the cap sign filter was set to $5e^{-7}$ $ms*v/m^2$ with a slope of -0.5 for the low moment and $2e^{-7}$ $ms*v/m^2$ with a slope of -0.5 for the high moment. The cap slope filter removed four time gates before the change in sign for both moments. The cap slope filters use the same time period, noise level, and noise slope as the cap sign filter and culls sounding data if the second order derivative of the dB/dt curve is outside of the minimum and maximum slope. The minimum slope was -0.5 and the maximum was 0.5 for both moments. The average sign filter works on the averaged data, removing data when a change in sign occurs. The average slope filters were not used on this data set. The trapezoidal filters are used to average the AEM sounding data. The times used to define the trapezoidal filters for the low moment are $1e^{-5}$, $1e^{-4}$, and $1e^{-3}$ with widths of 2, 5 and 10 seconds. The times used to define the trapezoid for the high moment are $1e^{-4}$, $1e^{-3}$ and $1e^{-2}$ with widths of 5, 10, and 20 seconds. The spike factor and minimum number of gates were both set to 25 percent for both soundings.

Manual Processing and Laterally Constrained Inversions

After the implementation of the automatic filtering, the AEM data were examined manually by using a sliding 2-minute time window. The data were examined for possible coupling with surface and buried metal as well as for late time gate noise levels. Data impacted by these were removed. In addition, the results of the automatic filtering processes were monitored. In some instances, AEM data that were removed by the automatic filters were re-included.

The AEM data were then inverted using a laterally constrained inversion (LCI) algorithm (Auken and Christiansen, 2004). A starting model consisting of 19 layers with starting resistivities of 40 ohm-m were used. This model went to a depth of 300 meters with the thickness of the layers increasing with depth. The vertical resistivity standard deviation was set to 2, while the lateral resistivity standard deviation was set to 1.3 for the first 11 layers, 1.25 for layers 12 through 15, and 1.2 for layers 16 through 19. Following the LCI, profile and depth slices were created to examine the results of the inversion. When remaining couplings were located the data were again manually removed and additional LCIs were performed.

Spatially Constrained Inversion

If the results of the second LCI were determined to be free of couplings, a spatially constrained inversion (SCI) (Viezzoli and others, 2008) was performed on the data. The starting model and standard deviations used were the same as those described for the LCI. Additionally the SCI creates sections in which the inversions are spatially constrained. The approximate section size selected was 100 soundings, with a minimum of 50.

The inversion results were once again examined using profiles and depth slices. If any remaining coupling were detected they were removed and the inversions run again. The resulting models are then exported from the Workbench as ASCII file formats.

Data display and interpretation

The interpretation of the AEM inversion resistivity model was completed in a Geographical Information System (GIS) that provided X, Y, and Z coordinates (PitneyBowes, 2013). Prior to interpreting the AEM data, several complementary datasets were included and graphically displayed in 2-D and 3-D GIS environments. Complementary data included test-hole lithology, test-hole geophysical logs (including natural gamma and electrical resistivity), TDEM resistivity models, airborne measurements of the intensity of 60-hertz power-line interference, airborne measurements of the magnetic total-field intensity, airborne photographs, and the 90-m digital elevation model (DEM). Other maps, identifying roads, power lines, pipelines, towns, and geology, were used. The AEM inversions were displayed as colored resistivity sections within the GIS environment. The resistivity data were plotted using the same color scale, and all of the datasets were placed in the same projected coordinate system. This allowed the data to be examined at many scales and for data to be interactively displayed and/or hidden in order to fully examine how the geophysical data interrelate with complementary datasets.

Hydrogeology of the Project Area

Physical Setting

The project area is underlain by a sequence of Quaternary-age deposits that overlie consolidated, Cretaceous-age sedimentary strata. The area is situated within Nebraska's Rolling Hills Topographic Region (CSD, 1973). This physiographic setting is predominately a hilly upland landscape with moderate to steep slopes and rounded hilltops. The hills in the area are composed of glacial till mantled by wind-transported silt deposits (loess). Local relief within the project area can exceed 30 meters between hilltops east of Clarkson and the West Maple Creek valley. The groundwater system in the project area falls within the CSD's Nebraska Glacial Drift Groundwater Region classification. The most prolific aquifers in this setting are composed of buried coarse sediments. In areas where these sediments are not present, groundwater development occurs where isolated pockets of groundwater occupy the void spaces of coarse-grained deposits that overlie glacial till (CSD, 1998).

Surface Hydrology

The upland area east of Clarkson is dissected by small drainages that slope locally into West Maple and East Maple Creeks (Figure 1). The parallel valleys of West and East Maple Creeks are oriented northwest to southeast and reach confluence at Maple Creek in southwest Dodge County before emptying into the Elkhorn River north of Fremont, Nebraska. No stream gage data for West or East Maple Creek is available within or near the project area. A USGS stream gage (06800000) on the main stem of Maple Creek near Nickerson, Nebraska has an average annual flow of 2.3 cubic meters per second between 1952 and 2004 (Fredrick and others, 2006). The steeply sloped catchments in the survey concentrate runoff, providing potential recharge to the groundwater flow system. There are numerous small stock ponds, terraces and stream channelization in the project area, which affect runoff and potential recharge.

Geologic Setting

Quaternary Geology

Groundwater resources currently used for municipal, domestic, and irrigation purposes in the project area are extracted solely from unconsolidated sediments. These sediments were deposited along the southern edge of the Laurentide Ice Sheet that advanced and retreated across northeast Nebraska during pre-Illinoian time of the Pleistocene Epoch (1.6 million to 300,000 years before present). The several hundred meter thick ice sheet (Dyke and others, 2002; Mathews, 1974) deposited till (unsorted geologic material ranging in size from clay to boulders) across eastern Nebraska. The glacial deposits in the project area are the result of the ice sheet overriding the soils and outcrops of the preglacial landscape. Where ice sheet movement stagnated, thick, extensive accumulations of till would result in remnant landform features known as moraines. During pre-Illinoian time, ice sheet advances resulted in at least four extensive moraine systems in eastern Nebraska. Reed and Dreezen (1965) recognized these moraine systems as controls on surface drainage patterns in eastern

Nebraska, including the flow divide that exists between Clarkson and Howells. In the project area, thick deposits of ōClarkson Tillö (Reed and Dreezen, 1965) are present along the northwest to southeast trending moraine that forms the present-day hummocky uplands between West and East Maple Creeks. CSD maps indicate that glacial till is at least 15 meters thick across the project area, and can exceed 45 meters in places, with the thickest areas found in the central portion and the southwest corner of the project area.

Sand and gravel deposits resulting from glacial melt water deposition are present at the base of the till and sit unconformably on the Cretaceous-age bedrock. These coarse materials are often intermixed with clay and silt, but can range from less than one meter to nearly 20 meters in composite thickness. However, the thickness and composition of the sediments underlying the till can vary considerably over short distances. In addition to the basal coarse materials, isolated lenses of coarse material within the till can supply limited quantities of water to low-capacity wells. The most extensive and continuous distributions of coarse deposits are found on the western edge of the moraine area along the modern-day West Maple Creek drainage and to a lesser extent on the east side of the project area southeast of Howells. Approximately 2.4 kilometers southeast of Clarkson, sand and gravel deposits exceed 25 meters in thickness.

The Laurentide Ice Sheet did not advance into eastern Nebraska during the Illinoian and Wisconsinan Epochs. However, the presence of the ice sheet east and north of the project area during this time altered climatic patterns to create persistent windy and dry conditions to the west. This resulted in transportation and deposition of loess (silt) across the region (Condra and Reed, 1959). In the project area, upwards of ten meters of loess can be present based on regional mapping (Mason and others, 2006). Locally, CSD test holes indicate nearly 15 meters of silt in the project area (CSD website, 2013). Based on regional reports, the surficial loess deposits are primarily Wisconsinan-age Peoria Loess (Muhs and others, 2008), which lies above older, Illinoian-age silt of the Loveland Formation in Colfax County (Bartlett and others, 1982).

Hydrogeology of Quaternary Deposits

The aquifer underlying the project area is comprised of sand and gravel deposits in the West and East Maple Creek drainages and includes the limited and dispersed coarse material scattered across the base of the upland till. Of less significance, isolated lenses of coarse sediments within the till sequence have limited storage and produce water to low-capacity wells across the project area.

The extensive distribution and thickness of fine-grained glacial and eolian deposits in the uplands between the West and East Maple Creek drainages creates semi-confined to confined conditions within the basal aquifer. Water levels in most wells screened in the lower coarse portion of the Quaternary sequence in the upland area typically have potentiometric head at elevations above the base of the fine material. The thick, fine sediment sequence also inhibits aerially extensive recharge from precipitation to the basal aquifer. The higher rates of recharge to the groundwater system occur in the valley areas where coarse deposits are relatively close to the land surface. These areas can also provide recharge to the basal aquifer beneath the till in areas where there is adequate connectivity between the two intervals. Szilagyi and Jozsa (2013) estimated a net recharge to

groundwater ranging from 0 to 25 millimeters based on calculations from a statewide water balance modeling study. The maximum value of this range (25 millimeters) equates to approximately 3.5 percent of annual precipitation.

Records from the Nebraska Department of Natural Resources (NDNR) Registered Well Database indicate considerable variability in aquifer productivity across the project area. The NDNR database has 101 registered well records within the project area. Of the registered wells, 49 have an associated pumping rate listed with an overall range of 0.04 to 7.6 m³/min. Within the project area, 17 registered domestic wells are in use with an average yield of 21 gpm. The database lists 32 irrigation wells, with an average rate of about 910 gpm. Figure 3 shows the location, depth and registered pumping rates for domestic, public supply and irrigation wells across the project area. It should be noted that these pumping rates have not been independently verified, and are likely to differ from when the well was originally constructed and registered. Irrigation wells are found

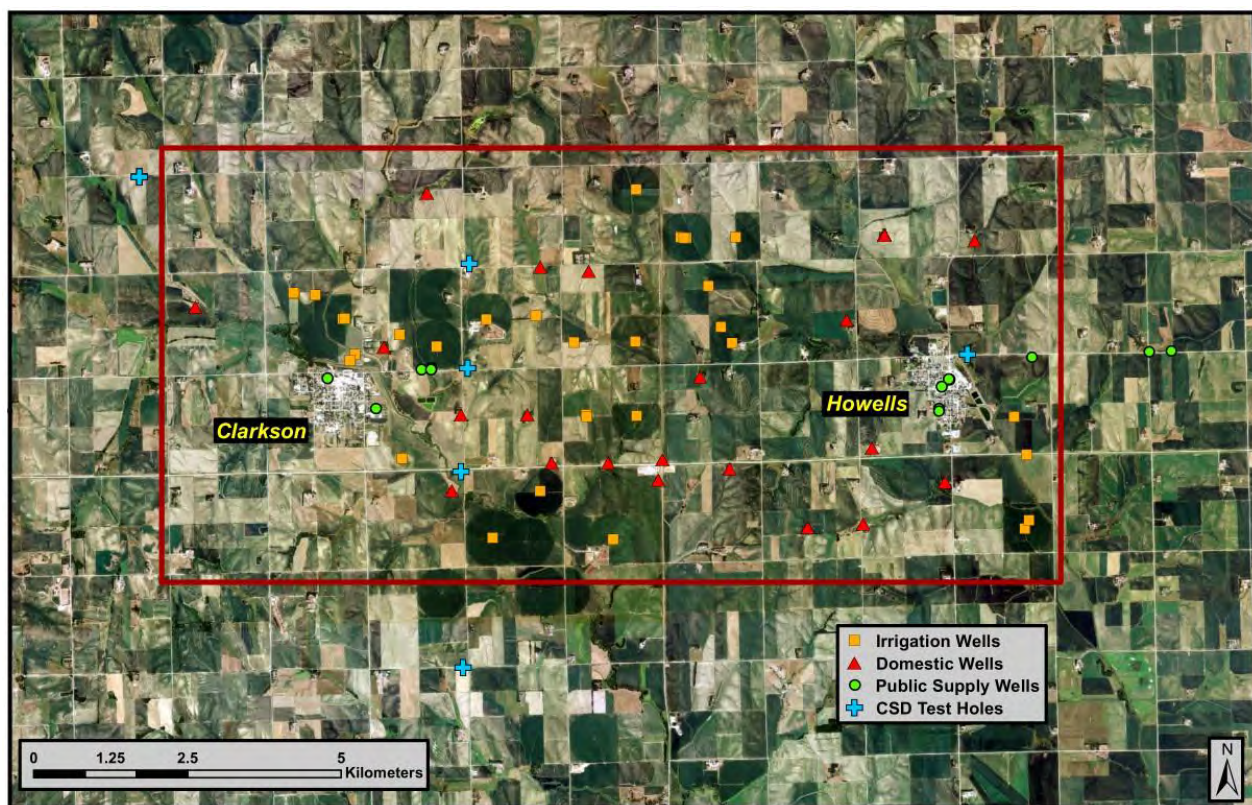


Figure 3 – Locations of registered wells by use and CSD test holes in the Project Area.

primarily in the mid-section of the project area and near Clarkson, with a noticeable absence of high-capacity wells in the eastern one-third of the project area and in the area south and west of Clarkson. The patterns of well uses and rates provide a qualitative inference into the overall extent of productive aquifer materials in the project area. High-capacity wells require a certain level of areal extent and thickness of coarse sediments to maintain long-term productivity, whereas low-capacity wells typically used for domestic or livestock purposes can utilize smaller, isolated zones of coarse materials and still remain

productive. In some instances, such as at registered well numbers G-119259 and G-122916, low-capacity wells are screened over entire intervals of fine deposits with limited or no coarse material and still yield small flow rates.

In 2012, Nebraska experienced one of the severest droughts since the Dust Bowl of the 1930s, including the driest July-September period on record (www.climatecentral.org). The LENRD provided XRI spring water level measurements from 2008-2013 at five locations within or near the project area. At these five locations, water levels declined between April 2012 and April 2013 by an average of 4.6 meters (Figure 4). Over calendar year 2012, the average of two observed precipitation totals from different sources near Clarkson was

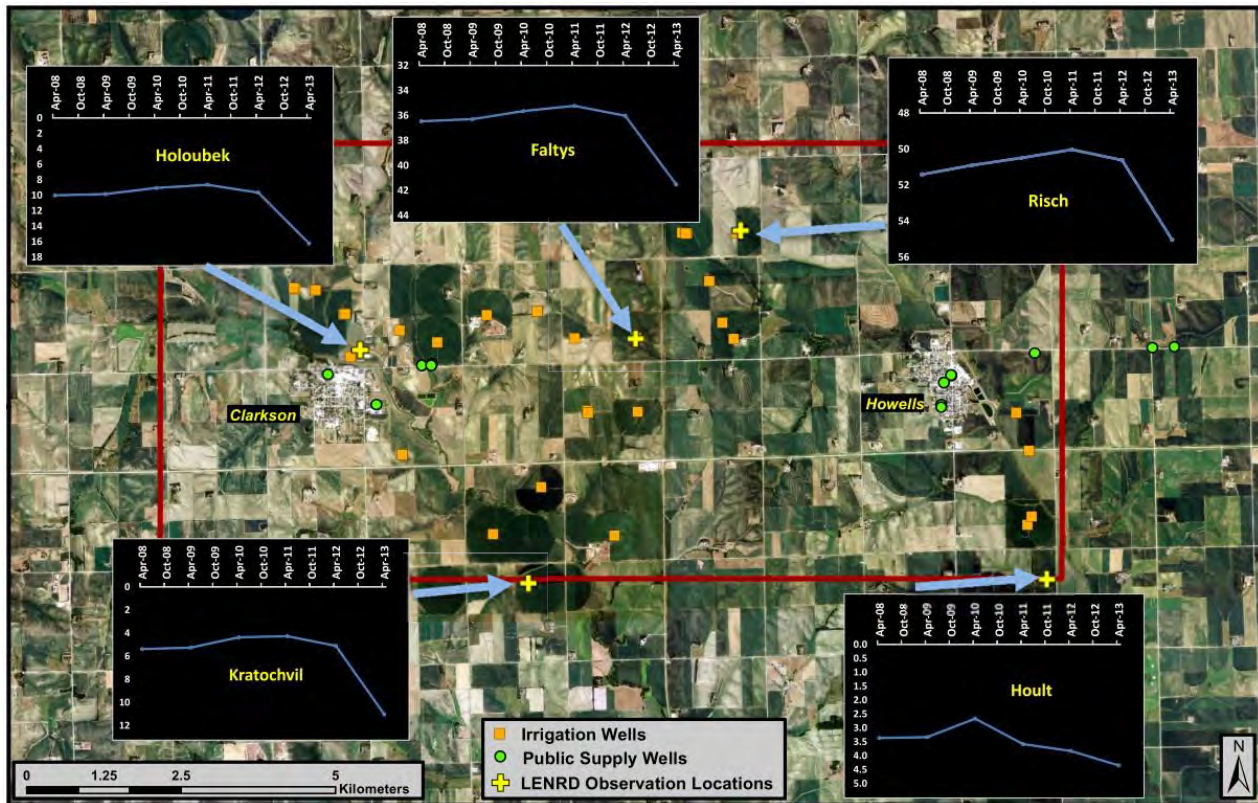


Figure 4 – Observed water levels at five locations provided by the Lower Elkhorn NRD for the 2008-2013 time period. Note the water levels are in meters below ground surface, and the scale of the y-axis differs by location.

373.4 millimeters, which was 337.8 millimeters below the average annual precipitation rate of 711 millimeters (NeRain website, High Plains Climate Center). The near 50 percent departure in average annual precipitation and the corresponding response in the water table across the project area demonstrates that the aquifer is limited in volume and extent and is vulnerable to drought in glaciated terrain. With the record low precipitation during the highest crop water use months from July through September, it is highly likely that irrigators produced more water from wells than in a normal precipitation year. This added stress on the described limitations of the glacial aquifer system, and it is not unexpected to see these declines recorded in the water level record.

Cretaceous Geology and Aquifer Potential

Beneath the Quaternary deposits in the project area is a sequence of sedimentary strata that were deposited when the region was inundated by the mid-continent seaway during the Cretaceous Period (65 to 130 million years ago). As the seaway transgressed and regressed across present-day Nebraska, varying sedimentary rock types were deposited, including marine shale, limestone, and sandstone. The rock type and thickness are a function of the depth of the seaway and proximity to the shoreline of the sea in the area. Carlile Shale underlies most of the project area, along with a small portion of Greenhorn Limestone and Graneros Shale beneath the southeast quarter of the project area (Burchett, 1986). The outcropping and near-surface portions of these formations were subject to extensive weathering, degradation and erosion during the Quaternary period. As the continental ice sheet extended across the area, the abrasive power of the ice altered and eroded the land surface, leaving the upper most strata thin and likely absent in some locations. None of these formations are known to produce beneficial amounts of potable water in the region. Directly above the contact with the Cretaceous formations there is a thin coarse zone of terrestrial sediment.

Below the Carlile, Greenhorn, and Graneros is the Dakota Group, which is comprised predominately of sandstone interbedded with shale and is utilized as an aquifer in many areas of eastern Nebraska. The nearest wells in the region that utilize the Dakota Group are located about 16 kilometers southeast of Howells in west-central Dodge County (NDNR, 2013). These wells have yields ranging from 800 to 1,000 gpm. Water quality from these wells is unknown.

Very little data exists on the character of the Dakota Group immediately within the project area and the LENRD. However, as Dakota sandstone is regionally extensive, the wells in Dodge County provide an example of a potential aquifer that may have importance to the LENRD. Exploratory wells along with proper data collection on aquifer characteristics could provide information into the potential yield and water quality characteristics of the sandstone. If conditions are suitable, the Dakota Group sandstone could serve as a new aquifer resource in the Clarkson-Howells area.

Interpretation of AEM Results

Map of the Principal Aquifer

The AEM resistivity model reveals the character of the Quaternary deposits across the project area with a level of three-dimensional detail that would be unobtainable with the current inventory of borehole information. Interpretive imagery from the AEM survey are presented in Appendix 1, and each figure in the appendix will be denoted with the letter A. Output generated from the survey (Figures A-1 and A-2) shows distinct contrasts between electrically conductive materials (clay and silt) and more electrically resistive sediments (coarse deposits). The conductive zones are interpreted as glacial till and loess, whereas the resistive areas indicate the extent and thickness of the principal aquifer (hereafter referred to as "aquifer") in the project area. There is no evidence in the historical work that saline water is present in the survey area, which would cause the electrical conductivity to increase. The geologic descriptions from borehole logs across the area match the

geophysical results well, although deviations occur in some areas as most boreholes are not located directly along a survey flight-line. In addition to the Quaternary deposits, the character of the bedrock surface has been isolated to display the subsurface topography beneath the Quaternary system (Figures A-3 and A-4). The subsurface topography is directly related to the advance and subsequent erosion created by the ice sheet.

The principal aquifer can be delineated with various thresholds of resistivity, as displayed in Figures A-5 through A-11. Higher resistivity values correspond to areas in the subsurface with greater potential for productive aquifer materials. The overall spatial extent of the aquifer is apparent at the 15 ohm-m level, however, the 20 ohm-m level and above represent areas where there is greater confidence in the location of the principal aquifer. The largest resistivity values detected in the survey underlie the modern-day valley of West Maple Creek from Clarkson southeastward to the project area boundary. Figure A-2 (a 3-D voxel) shows the extent of this resistive area with a horizontal slice removed from the uppermost surface of the geophysical data. These deposits are clearly evident at the 25 ohm-m and greater level (Figure A-10). In this area, resistive materials exceed 30 meters in thickness and are encountered at relatively shallow depths across an area 2.5 kilometers in width west to east. This deposit narrows and thins northwest of Clarkson into isolated lenses exhibiting resistivity values less than 20 ohm-m.

Beneath the upland till area between Clarkson and Howells, coarse deposits indicated by the 20 ohm-m and above threshold are limited to discontinuous zones layered between the glacial till and the underlying Cretaceous bedrock (Figures A-7 and A-8). These resistive units are typically less than 10 meters thick and cover areas less than one square kilometer, with the most isolated areas found in the northern half of the project area. The thickest portion of resistive material in this area lies north of Road X, approximately 1.5 and 4 kilometers west/northwest of Howells. This pocket of resistive material ranges from 20 to over 30 meters in thickness. Borehole data from this area further supports the geophysical results by matching the geology to the resistivity model. In the Howells area, thin resistive units underlying the East Maple Creek valley are present on the eastern edge of the town and extend southward to the project area corner. The range in thickness of resistive sediments is from 12 to 15 meters in this area. A brief review of borehole logs from the NDNR Registered Well Database located immediately east of the project area indicates that overall thickness of this resistive interval decreases eastward. Thus, the resistive unit on the southeast edge of the project area is likely not associated with a more productive aquifer beyond the project area boundary.

In summary, the principal aquifer in the project area is limited in both thickness and extent. The thickest detected aquifer materials underlie the West Maple Creek valley south of Clarkson. East of Clarkson, aquifer materials beneath the thick upland till are generally thinner, discontinuous, and in many locations, completely absent. The most extensive interval of coarse deposits beyond the West Maple Creek area is located west/northwest of Howells where more than 30 meters of resistive material was detected. The resistors seen at the 20 ohm-m level are no longer seen at the 25 ohm-m level because they are such poor resistors and are masked (Figures A-9 through A-11). This demonstrates the discontinuous nature of the principal aquifer beneath the upland till. In the far eastern extent of the project area, a thin resistive zone is present to the east and southeast of Howells beneath the East

Maple Creek valley. Figures A-12 through A-17 show cross-sectional slices of the geology along six different flight lines. These cross sections further demonstrate the limited extent of the principal aquifer in the project area.

Estimate of Aquifer Volume

Three-dimensional digital representation of the subsurface resulting from the AEM method provides users the ability to more accurately estimate total aquifer volume and the amount of extractable water. For this calculation, the 15 ohm-m threshold is used to separate aquifer from non-aquifer materials with any value below 15 ohm-m to be considered non-aquifer material. As described previously in this report, the higher a material's resistivity the more likely it is to be an aquifer. Therefore, a progressive assumption is made between the 15, 20, and 25 ohm-m thresholds, with each having a larger specific yield value (0.10, 0.12 and 0.15, respectively). In absence of any historical data on specific yield, these values were selected as conservative estimates of the storage capacity of the aquifer. A majority of the borehole logs indicate the presence of clay and silt within the sand and gravel, a condition that would be expected in glacial outwash and is another reason for the selected specific yields. The total volume extractable water calculated by using the previous assumptions is slightly over 131 million cubic meters (Table 1).

Table 1. Estimates of extractable water content in the principal aquifer underlying the Project Area.

Resistivity Threshold (ohm-m)	Aquifer Volume (m ³)	Specific Yield	Extractable Water Volume (millions m ³)
15-20	7.3 x 10 ⁸	0.1	73.4
20-25	3.4 x 10 ⁸	0.12	40.3
25 and above	12 x 10 ⁸	0.15	17.8
TOTAL	1.2 x 10 ⁹		131.5

Relationship to Current Test Holes and Extraction Wells

Nearly 90 percent of the registered irrigation and domestic wells within the project area are located above the zone defined by the 15 ohm-m threshold limit and nearly half of these wells are within the 20 ohm-m threshold limit. Only six CSD test holes are present within the project vicinity, with a fifth located just beyond the northwest corner of flight line block. XRI assessed the lithology of each of these test holes and assigned Unified Soil Classification System soil descriptor codes to each unique lithologic interval. The same process was repeated for the registered well borehole logs. It should be noted, however, that the quality of the borehole logs from the registered wells varies greatly from log to log and were not subject to the same quality assurance and quality control as the CSD logs. The log data from all sources was compiled and included in the AEM processing software for overlay comparison with the geophysical results.

Figure 5 below show examples of the borehole lithology compared to the AEM results along the west-east flight-line south of Clarkson. The comparison of the boreholes and the geophysical results match closely. It should be noted that very few well or test hole

locations are directly on a flight-line, and that slight deviation should be expected between the borehole lithology and the geophysical information due to the inherent complexity of glacial depositional environments.

In a limited portion of the project area, disagreement exists between the geophysical data and the borehole lithologic descriptions. Northeast of Clarkson and north of Road X, a band of irrigation wells aligned west to east do not lie within the 15 ohm-m zone. The geophysical information does not reveal the thickness of the sand and gravel deposits described in the lithologic logs, including those from a recent CSD test hole 02-LE-13. The flight line is located approximately 50 meters from the test hole 02-LE-13. Using the well log resistivity data (16 inch normal) collected by CSD a forward model was calculated for the AEM system response. The forward model was then inverted using the same settings as used for the inversion of the Clarkson AEM data. The inversion of the forward model detected the resistive sands and gravels as indicated in the well log (Figure 6). This exercise indicated that in order to detect these small areas of sand and gravel a line spacing of 100 meters or less would have been required.

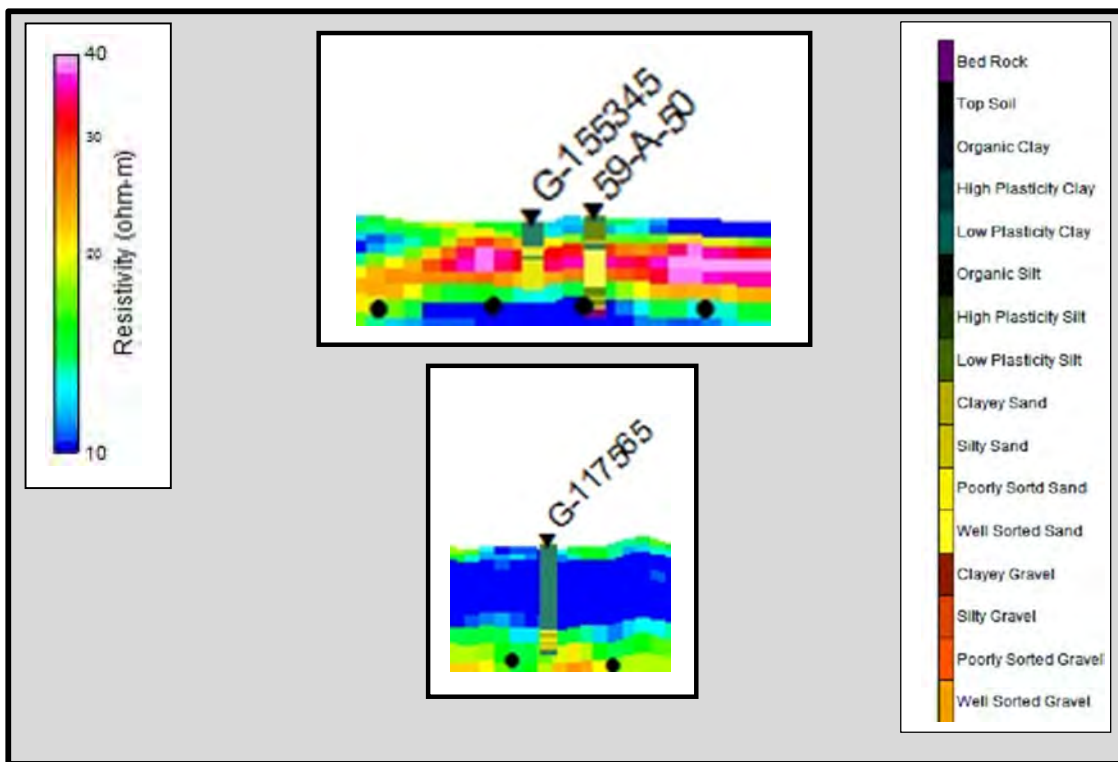
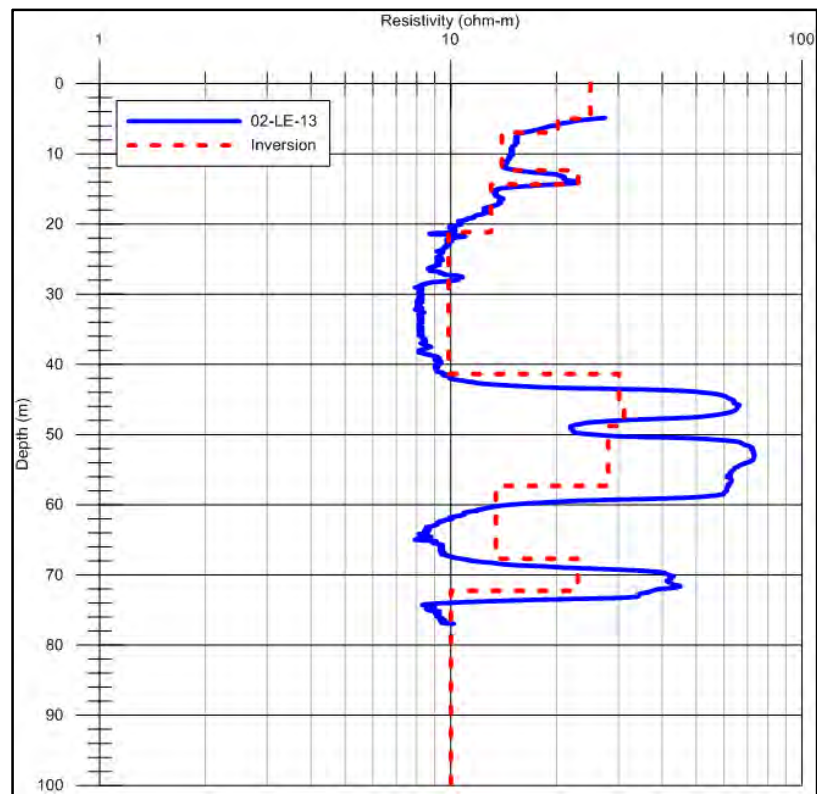


Figure 5 – Comparison of the subsurface resistivity (scale on the left) and the lithologic classifications at borehole log locations along the west to east fly-line south of Clarkson. Note that log 59-A-50 in the upper plot is a CSD test hole.

Figure 6 – Comparison of the resistivity values from test hole 16 inch normal log of 02-LE-13 (blue line) and an inverted forward modeled response from that log using the SkyTEM 304 system characteristics and inversion settings (red dashed line).



Each of these wells is registered to pump 3 cubic meters per minute (m^3/min) or greater, with very small reported drawdowns. This information from the NDNR database could be suspect, especially in consideration of the water level declines reported in the project area observation wells in April 2013 (Figure 4). Further investigation of borehole lithology logs from the NDNR database indicates the possibility that the irrigation wells are screened in a narrow deposit of coarse sediments, which flight line design failed to capture. Near the middle of this line of wells, well number G-128431 has nearly 19 meters of continuous sand and gravel deposits above the base of the hole. Less than 430 meters to the southeast, well G-137134 has a composite thickness of only 4.9 meters of sand and gravel that is interlayered with clay seams exceeding 2 meters in thickness. This example demonstrates how within the glaciated terrain of the project area, there is great variability in sediment characteristics within short distances, and in places within distances smaller than the resolution capabilities of the AEM data line spacing.

Estimated Potential Recharge Areas

Recharge to the groundwater flow system depends on multiple factors: precipitation rate, soil type, composition and thickness of the vadose zone, surface slope, density and type of vegetation, and land use practice. The greatest chance for recharge in the project area occurs in areas where the landscape is relatively flat and where the upper soil horizon and vadose zone allow for rapid infiltration and downward transmittal of water below the root zone. In the project area, the surface topography is considered to be the leading factor in dictating the location and rate of recharge, with the greatest potential existing in the valleys of West and East Maple Creeks. In these areas, the land surface is generally flat relative to

the upland hills between Clarkson and Howells. In these valleys, the most common soils are silt loams and silt-clay loams with high capacities for infiltration and water holding capacity (Bartlett and others, 1982). Although records of surface flows in West and East Maple Creeks are not available, it is possible that during periods of high precipitation and runoff, the coarse deposits in the valley could be recharged by direct infiltration of flow in the creeks if the water table is below the base of the creek beds.

In the upland areas, two factors limit the potential for recharge to reach the principal aquifer. First, the overall thickness of the till can exceed 40 meters in places. The combination of the depth to the principal aquifer and the low permeability of the till, limits the potential for water to reach the saturated zone within a time period suitable to replenish the aquifer after lengthy periods of pumping. Second, the overall surface slope in the upland areas enhances rapid runoff and reduces the potential for infiltration, except in catchment areas where runoff collects and does not immediately flow out of the area. The soils mapped in the upland areas have slopes typically ranging from 6 to 17 percent (Bartlett and others, 1982). Recharge can occur in isolated areas where erosion control practices concentrate runoff or reduce rapid overland flow with terraces, stock dams for small ponds, and channelized streams. The AEM survey detected isolated resistive materials on the tops of hills between Clarkson and Howells (Figure A-1). In these isolated areas, precipitation can infiltrate and later be transmitted to the surface drainages that dissect the hills. These very local, shallow systems are considered to be isolated from the principal aquifer in the project area.

In summary, the areas where highest recharge to the principal aquifer is likely to occur are the West and East Maple Creek valleys where the soil infiltration and storage capacity are high and the depth to the water table is relatively shallow. Recharge to the principal aquifer that underlies the upland till is limited to areas where the surface topography allows for runoff to collect and can slowly infiltrate through the till along preferential pathways. Local, shallow flow systems can occur on upland area hilltops as these areas exhibited slightly more resistive signatures in the AEM survey. These areas are not considered to be major sources of recharge to the principal aquifer.

Bedrock Aquifer Potential

The AEM technology used in this project allows for three-dimensional visualization of the unconsolidated Quaternary deposits and the upper Cretaceous bedrock underlying the project area. As described previously in the Cretaceous Geology section, several sedimentary bedrock units are present beneath the project area, including the Dakota Group, a bedrock aquifer resource utilized in many parts of eastern Nebraska. Although CSD bedrock geology maps indicate shale and limestone beneath the project area, the results of the AEM survey reveal elevated resistivity signatures in the uppermost 50 to 100 meters of bedrock that indicate Dakota Group sandstone immediately beneath the project area. It is likely the softer shales and limestones could have been partially excavated in the area by the abrasive forces of the Laurentide Ice Sheet during pre-Illinoian time.

The underlying bedrock identified by the AEM survey with resistivities corresponding to Dakota Group sandstone is located, along a northwest-southeast trend through the middle one-third of the project area (Figure A-18). Previous results from Abraham and others

(2011a) indicated that the sandstone portions of the Dakota group are detectable using time domain techniques. The highest detected resistivities are immediately west and southwest of Howells. Figure A-19 shows these resistive areas with an 18 ohm-m threshold with the more conductive portions of the bedrock faded. In this area, the bedrock sits beneath over 100 meters of Quaternary deposits. The relatively high resistive zones approach nearly 100 meters in thickness in the upper bedrock southwest of Howells, indicating the potential for a groundwater resource in this area. This area is apparent in the cross sectional slice of the subsurface in Figures A-13 and A-16. Although no Dakota Group wells exist within or in the immediate vicinity of the project area, irrigation wells in west-central Dodge County utilize the Dakota Group and yield between 2.6 and 3.8 m³/min according to NDNR database records. These wells are within 16 kilometers of the project area and indicate that there is potential for development from this bedrock resource as the Dakota Group aquifer is regionally extensive in eastern Nebraska. One concern that exists in using groundwater from the Dakota Group sandstone is the potential for poor water quality related to elevated levels of iron, manganese and total dissolved solids. Since the Dakota Group wells in Dodge County are used for irrigation, which require a certain level of water quality for healthy plant growth, the water quality of the Dakota Group in northern Colfax County could require little to no treatment. However, the quality of the bedrock aquifer water cannot be ascertained without sampling and analysis.

Summary and Recommendations

Recent drought conditions (2012) in the LENRD have shown that the project area between the towns of Clarkson and Howells have severe water supply problems that cannot be fully understood with current hydrogeologic information. For the LENRD to effectively utilize their groundwater management plan, detailed information on the area aquifer is necessary. In particular, the LENRD needs to understand the physical characteristics of the aquifer, the interconnection of the aquifer with surface water, the connectivity with adjacent aquifers, and the distribution of aquifer materials at the existing groundwater production wells. There are six (6) CSD test holes in or near the project area. These test holes are vital to the understanding of the area, but they cannot provide enough information to complete a detailed hydrogeologic framework.

AEM surveys were performed to supplement the testhole information in development of a new hydrogeologic framework of the project area. Traditional geologic information must be part of any AEM study, and it was included in the hydrogeologic framework generated for this project. The hydrogeologic framework developed from the AEM data was used to visualize the subsurface in three dimensions. A 3-D evaluation of the aquifer was made to estimate various percentages of the aquifer materials and their location/relationship to existing extraction wells, streams, and other aquifers. The primary aquifers in the area are small and of limited extent and are mostly confined to the West and East Maple Creek areas. There are numerous isolated deposits of aquifer materials that supply water to low yield wells across the project area. It is estimated that 131.5 million cubic meters of recoverable water is available in the aquifer materials underlying the project area.

The limited volume of groundwater in the small, discontinuous aquifers of the project area, combined with the impact of the drought in 2012 causing larger than normal pumping

volume from wells in the area (assumed) resulted in the precipitous water level declines observed in the project area. It is important to note that the return or continuation of drought conditions will most likely cause similar declines to the amount of water in storage. The limited areas identified in this study where aquifer recharge is expected to occur further restricts the sustainability of the aquifer during times of drought. The information provided herein will assist the LENRD in determining the rate of withdrawal from the aquifer during differing climatic conditions. The estimate of the amount of groundwater in storage balanced with allowable withdrawals can lessen the impact of climate variations.

An additional result from this work is the identification of potential water supply in the sandstones of the Cretaceous Dakota Group below the Quaternary deposits. It is recommended that additional work be done to determine the extent and character of this potential resource. The Dakota Group Sandstone is currently used for irrigation and water supply near the project area and it is possible for similar conditions to exist between Clarkson and Howells.

Bibliography

- Abraham, J.D., Bedrosian, Asch, T.H., Ball, L.B., Cannia, J.C, Philips, J.D., and Lackey, S. 2011a. Evaluation of Geophysical Techniques for the Detection of Paleochannels in the Oakland Area of Eastern Nebraska as Part of the Eastern Nebraska Water Resource Assessment: U.S. Geological Survey Scientific Investigations Report 2011-5228, p. 40. <http://pubs.usgs.gov/sir/2011/5228/>
- Abraham, J.D., Cannia, J.C, Bedrosian, P.A., Johnson, M.R., Ball, L.B., and Sibray, S.S. 2011b. Airborne Electromagnetic Mapping of the Base of the Aquifer in Areas of Western Nebraska: U.S. Geological Survey Scientific Investigations Report 2011-5219. <http://pubs.usgs.gov/sir/2011/5219/>
- Auken E., and Christiansen, A.V. 2004. Layered and laterally constrained 2D inversion of resistivity data, *Geoph.*, 69, 752-761, doi: 10.1190/1.1759461.
- Auken, E., Christiansen, A.V., Westergaard, J.H., Kirkegaard, C., Foged, N., Viezzoli, A. 2009. An integrated processing scheme for high-resolution airborne electromagnetic surveys, the SkyTEM system, *Explor. Geophys.*, 2009, 40, 1846192, doi:10.1071/EG08128.
- Aarhus Geophysics. 2013. Aarhus Workbench, version 4.1.1.765, <http://www.aarhusgeo.com/content/software/workbench/aarhus-workbench.html>
- Bartlett, P.A., Saeger, W.H., and S.K. Huso. 1982. Soil Survey of Colfax County, Nebraska. U.S. Department of Agriculture - Natural Resource Conservation Service and the University of Nebraska CSD.

- Burchett, R. R., 1986, Geologic Bedrock Map of Nebraska: Nebraska Geological Survey. Scale 1:1 million.
- Christiansen A.V., and Auken, E. 2012. A global measure for depth of investigation, *Geoph*, 77, 171-177, doi:10.1190/geo2011-0393.1.
- Christiansen, A.V., Auken, E., and Viezzoli, A. 2011. Quantification of modeling errors in airborne TEM caused by inaccurate system description, *Geoph.*, 76, 43-52, doi:10.1190/1.3511354.
- ClimateCentral.org. A Record Lack of Rain in Drought-Stricken Nebraska. October 5th, 2012. Accessed at <http://www.climatecentral.org/blogs/chart-shows-rainfall-record-in-drought-stricken-nebraska-15121> on December 7, 2013.
- Condra, G.E. and E.C. Reed. 1959. The Geologic Section of Nebraska. Nebraska Geological Survey Bulletin No. 14A.
- Dyke, A.S., Andrews, J.T., Clark, P.U., England, J.H., Miller, G.H., Shaw, J., and J.J. Veillette. 2002. The Laurentide and Innuitian Ice Sheets during the Last Glacial Maximum. *Quaternary Science Reviews*. Vol. 21, No 9-31.
- Eberhart-Phillips, D., Stanley, W.D., Rodriguez, B.D., and Lutter, W.J. 1995. Surface seismic and electrical methods to detect fluids related to faulting: *Journal of Geophysical Research*, v. 100, no. B7, p. 12919-12936.
- Fitterman, D. V., and M. Deszcz-Pan. 1998. Helicopter EM mapping of saltwater intrusion in Everglades National Park, Florida: *Exploration Geophysics*, 29, 240-243, doi: <http://dx.doi.org/10.1071/EG998240>.
- Foged, N., Auken, E., Christiansen, A. V. and Sørensen, K. I. 2013. Test site calibration and validation of airborne and ground based TEM systems. *Geoph.*, 78, 95-106. doi: 10.1190/geo2012-0244.1.
- Fredrick, B.S., Linard, J.I. and J.L. Carpenter, 2006. Environmental Setting of Maple Creek Watershed, Nebraska. U.S. Geological Survey Scientific Investigations Report 2006-5037.
- HydroGeophysics Group, Aarhus University, Denmark, GUIDELINE AND STANDARDS FOR SKYTEM MEASUREMENTS, PROCESSING AND INVERSION, November 2011, version 2.5., <http://www.hgg.geo.au.dk/rapporter/SkyTEMGuideEN.pdf>
- HydroGeophysics Group, Aarhus University, Denmark, GUIDELINE AND STANDARDS FOR SKYTEM MEASUREMENTS, PROCESSING AND INVERSION, November 2011, version 2.5., <http://www.hgg.geo.au.dk/rapporter/SkyTEMGuideEN.pdf>

- HydroGeophysics Group. 2010. Aarhus University, Denmark, Validation of the SkyTEM system at the extended TEM test site, 2010, http://www.hgg.geo.au.dk/rapporter/Validating_SkyTEM_Test_Site_2010.pdf
- High Plains Climate Center. Clarkson, Nebraska Historical Data Summary ó 1940 to 2004 Average Annual Precipitation. Accessed at <http://www.hprcc.unl.edu/data/historical/> on December 7, 2013.
- Jørgensen, F, Scheer, W, Thomsen, S, Sonnenborg, T.O., Hinsby, K., Wiederhold, H., Schamper, C., Burschil, T., Roth, B., Kirsch, R., and Auken. E. 2012. Transboundary geophysical mapping of geological elements and salinity distribution critical for the assessment of future sea water intrusion in response to sea level rise: *Hydrol. Earth Syst. Sci.*, 16, 1845-1862, doi: <http://dx.doi.org/10.5194/hess-16-1845-2012>
- Jørgensen, F., Sandersen, P.B.E., Auken, E. 2003. Imaging buried Quaternary valleys using the transient electromagnetic method, *J. Appl. Geophys.*, 53, 199- 213, doi:10.1016/j.jappgeo.2003.08.016.
- Keller, G.V. 1987. Rock and mineral properties, in Nabighian, M.N., ed., *Electromagnetic methods in applied geophysics theory*: Tulsa, Oklahoma, Society of Exploration Geophysicists, v. 1, p. 13-51.
- Keller, G.V. 1989. Electrical properties, in Carmichael, R.S., ed., *Practical handbook of physical properties of rocks and minerals*: Boca Raton, Florida, CRC Press, 359-427.
- Lawrie, K.C., Brodie, R.S., Tan, K.P., Gibson, D., Magee, J., Clarke, J.D.A., Halas, L., Gow, L., Somerville, P., Apps, H.E., Christensen, N.B., Brodie, R.C., Abraham, J., Smith, M., Page, D., Dillon, P., Vanderzalm, J., Miotlinski, K., Hostetler, S., Davis, A., Ley-Cooper, A.Y., Schoning, G., Barry, K. and Levett, K. 2012. BHMAR Project: Data Acquisition, processing, analysis and interpretation methods. *Geoscience Australia Record* 2012/11. 826p.
- Mason, J. A., Bettis, A. E., Roberts, H. M., Muhs, D. R., and Joeckel, R. M., 2006, Last glacial loess sedimentary system of eastern Nebraska and western Iowa; AMQUA post-meeting field trip no. 1; *in*, Guidebook of the 18th Biennial Meeting of the American Quaternary Association, R. Mandel, ed.: Kansas Geological Survey, Technical Series 21, p. 1-161-22.
- Mathews, W.H. 1974. Surface Profiles of the Laurentide Ice Sheet in its Marginal Areas. *Journal of Glaciology*. Vol. 13, No. 7.
- Møller, I., Søndergaard, V.H., Jørgensen, F., Auken, E., and Christiansen, A.V. 2009. Integrated management and utilization of hydrogeophysical data on a national scale, *Near Surf. Geophys.*, 7, 647-659, doi:10.3997/1873-0604.2009031.

- Muhs, D.R., Bettis III, E.A., Aleinikoff, J.N., McGeehin, J.P., Beann, J., Skipp, G., Marshall, B.D., Roberts, H.M., Johnson, W.C. and R. Benton. 2008. Origin and paleoclimate significance of late Quaternary loess in Nebraska, Evidence from stratigraphy, chronology, sedimentology, and geochemistry. Geological Society of America Bulletin, November/December 2008.
- Nebraska Department of Natural Resources Registered Well Database. Accessed on December 7 and 8, 2013 at <http://dnrdata.dnr.ne.gov/wellscs/Menu.aspx>.
- Nebraska Rainfall Assessment and Information Network (NeRAIN). 2012 Observations in the LENRD. Accessed at <http://nerain.dnr.ne.gov/> on December 7, 2013.
- Nelson, P.H., and Anderson, L.A. 1992. Physical properties of ash flow tuff from Yucca Mountain, Nevada: Journal of Geophysical Research, v. 97, no. B5, p. 82366841.
- Oldenborger, G.A., Pugin, A.J.-M., and Pullan, S.E. 2013. Airborne time-domain electromagnetics, electrical resistivity and seismic reflection for regional three-dimensional mapping and characterization of the Spiritwood Valley Aquifer, Manitoba, Canada, Near Surf. Geophys., 11, 63-74, doi:10.3997/1873-0604.2012023.
- Paine, J.G., and Minty, B.R.S. 2005. Airborne hydrogeophysics, Hydrogeoph, 50, 333-357, doi:10.1007/1-4020-3102-5_11.
- Palacky, G.J. 1987. Resistivity characteristics of geologic targets, in Nabighian, M.N., ed., Electromagnetic methods in applied geophysics theory: Tulsa, Oklahoma, Society of Exploration Geophysicists, v. 1, 53-129.
- PitneyBowes. 2013. Encom Profile PA Analyst Software, Version 12.0.0, <http://www.encom.com.au/template2.asp?pageid=16>
- Reed, E.C. and V.H. Dreezen. 1965. Revision of the classification of the Pleistocene deposits of Nebraska. Nebraska Geological Survey Bulletin No. 23. 65 p.
- Sørensen, K., and Auken, E. 2004. SkyTEM - A new high-resolution helicopter transient electromagnetic system, Explor. Geoph, 35, 1916199, doi: 10.1071/EG04194.
- Szilagy, J., and J. Jozsa. 2013. MODIS-Aided Statewide Net Groundwater-Recharge Estimation in Nebraska. Groundwater. Vol. 51, No. 5.
- University of Nebraska-Lincoln Conservation Survey Division. 1973. State of Nebraska Topographic Regions Map. Accessed online at: <http://digitalcommons.unl.edu/cgi/viewcontent.cgi?article=1062&context=caripubs> on December 3, 2013.
- University of Nebraska-Lincoln Conservation Survey Division. 1998. The Groundwater Atlas of Nebraska. Resource Atlas No. 4a/1998.

University of Nebraska-Lincoln Conservation Survey Division Online Statewide Test Hole Database. Accessed multiple events in November 2013. Accessible at: <http://snr.unl.edu/data/geologysoils/NebraskaTestHole/NebraskaTestHoleIntro.asp>.

University of Nebraska-Lincoln Conservation Survey Division. State of Nebraska Glacial Till Deposit Map. Accessed online at: <http://snr.unl.edu/data/geographygis/NebrGISgeology.asp#till>

Viezzoli, A., Jørgensen, F., and Sørensen, C. 2013. Flawed Processing of Airborne EM Data Affecting Hydrogeological Interpretation: Groundwater, 51, No. 2, 1916202, doi: <http://dx.doi.org/10.1111/j.1745-6584.2012.00958.x>

Viezzoli, A., Christiansen, A.V., Auken, E., and Sørensen, K. 2008. Quasi-3D modeling of airborne TEM data by spatially constrained inversion, Geoph., 73, 105-113, doi:10.1190/1.2895521.

Viezzoli, A., Tosi, L., Teatini, P. and Silvestri, S. 2010. Surface water-groundwater exchange in transitional coastal environments by airborne electromagnetics: The Venice Lagoon example, Geoph. Res. Lett., 37, L01402, doi:10.1029/2009GL041572.

Wynn, J. 2002. Evaluating groundwater in arid lands using airborne magnetic/EM methods. An example in the southwestern U.S. and northern Mexico, The Leading Edge, 21, 62-64, doi:10.1190/1.1445851.

Appendix 1- AEM Interpretive Imagery

List of Figures in Appendix 1

- Figure A-1: 3-D voxel of all Quaternary deposits above bedrock.
- Figure A-2: 3-D voxel of all Quaternary deposits above bedrock with a horizontal clip in the southwest quarter of the project area.
- Figure A-3: Cretaceous bedrock topography beneath Quaternary deposits.
- Figure A-4: 3-D display of Cretaceous bedrock topography beneath Quaternary deposits.
- Figure A-5: 15, 20, and 25 ohm-m resistivity surfaces overlying the Cretaceous bedrock surface.
- Figure A-6: 3-D voxel display of 15 ohm-m or greater resistivity zones overlying the Cretaceous bedrock surface.
- Figure A-7: Areas of subsurface exhibiting resistivity at 20 ohm-m or greater overlying the Cretaceous bedrock surface.
- Figure A-8: 3-D voxel display of 20 ohm-m or greater resistivity zones overlying the Cretaceous bedrock surface.
- Figure A-9: Areas of subsurface exhibiting resistivity at 25 ohm-m or greater overlying the Cretaceous bedrock surface.
- Figure A-10: 3-D voxel display of 25 ohm-m or greater resistivity zones overlying the Cretaceous bedrock surface.
- Figure A-11: Thickness of principal aquifer area with resistivity levels at 25 ohm-m or greater.
- Figure A-12: West to East cross section along the southern tie-line.
- Figure A-13: West to east cross section along the middle tie-line.
- Figure A-14: West to East cross section along the northern tie-line.
- Figure A-15: South to north cross section along a flight line east of Clarkson.
- Figure A-16: South to North cross section along a flight line east of Clarkson and west of Howells.
- Figure A-17: South to north cross section along a flight line west of Howells.
- Figure A-18: Resistivity of the Cretaceous bedrock units beneath the Quaternary system and principal aquifer.
- Figure A-19: 3-D cloud display image of 18 ohm-m voxel in the Cretaceous bedrock underlying the Quaternary System and principal aquifer.

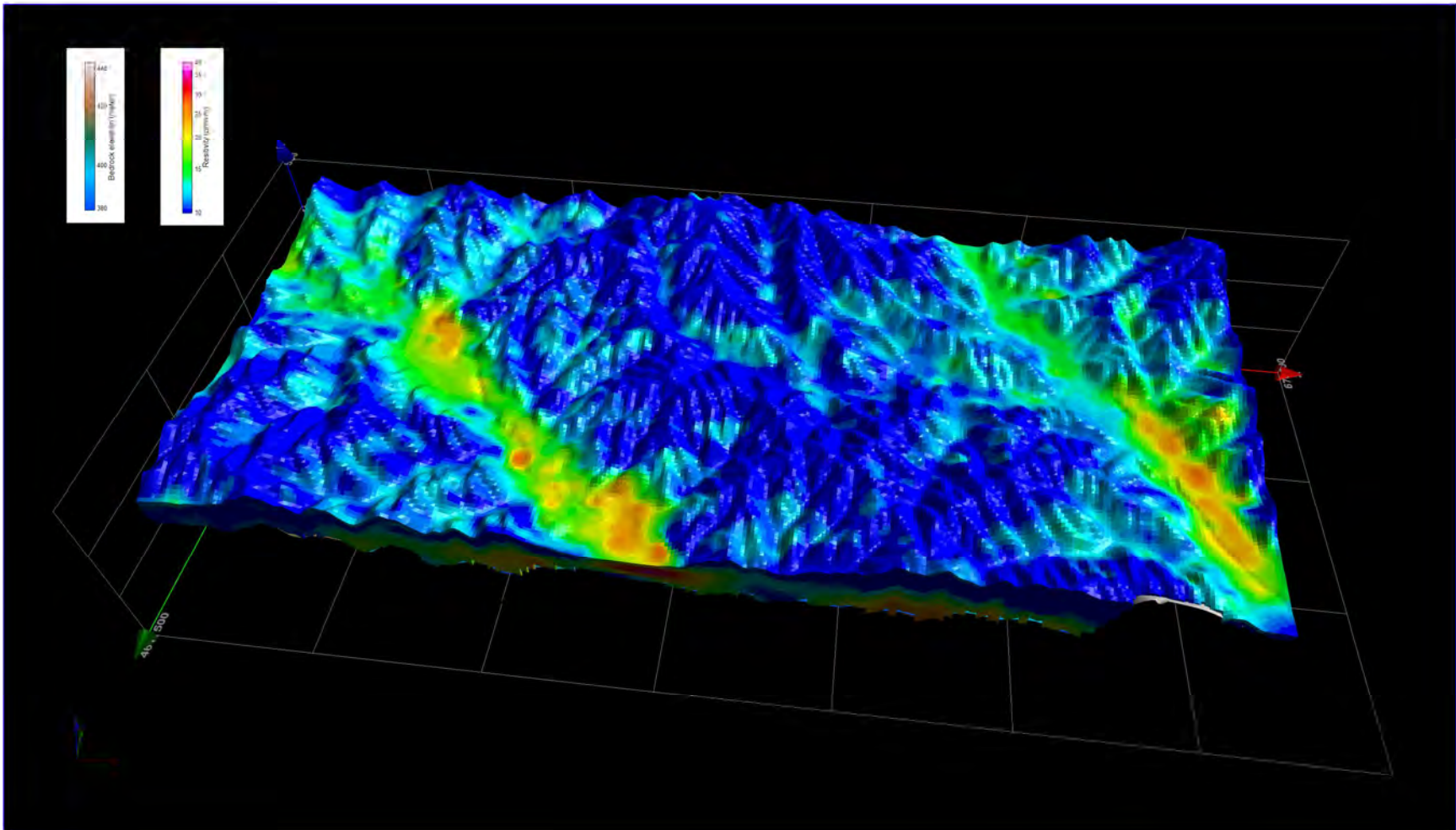


Figure A-1 – 3-D voxel of all Quaternary deposits above bedrock.

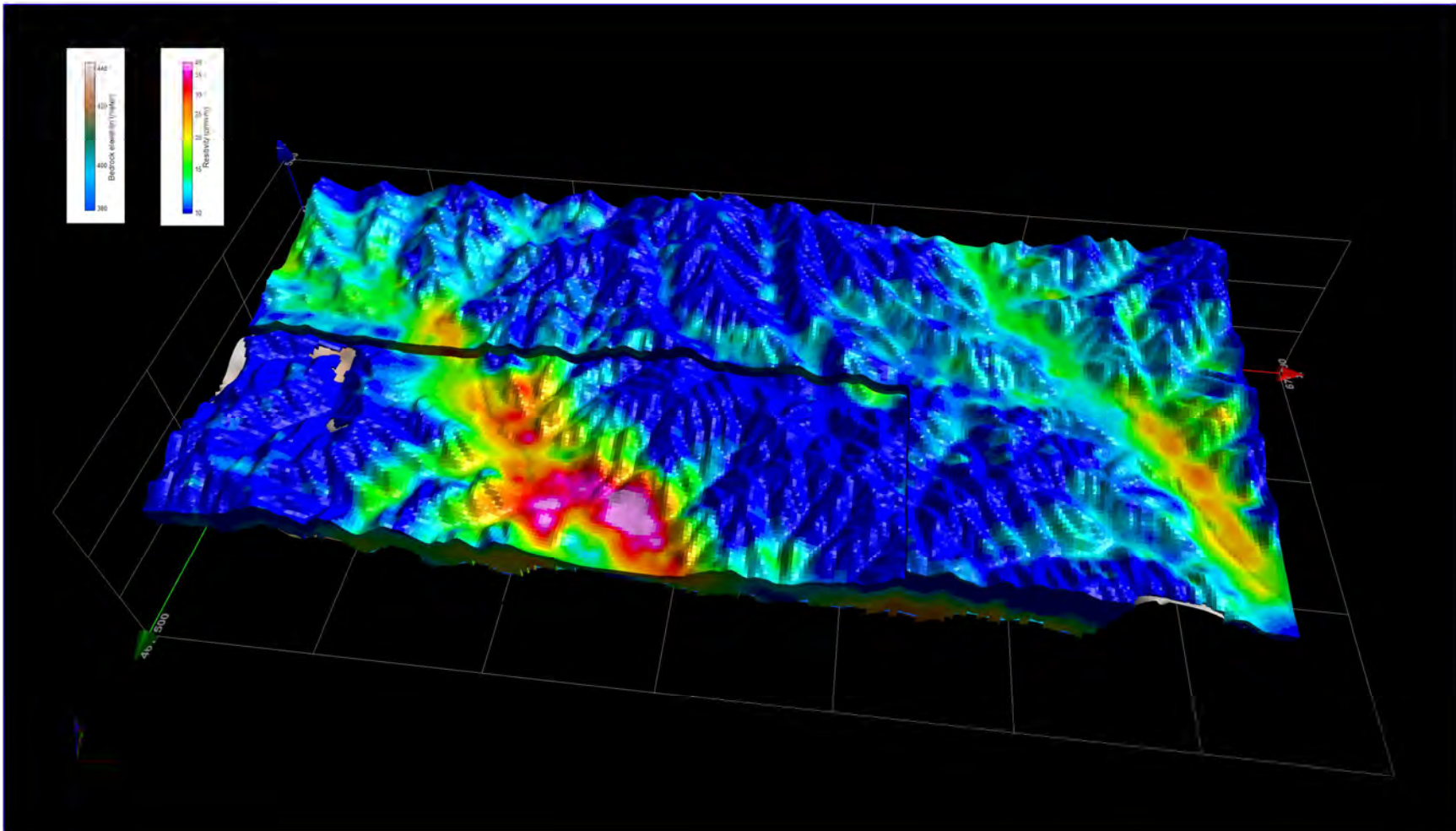


Figure A-2 – 3-D voxel of all Quaternary deposits above bedrock with a horizontal clip in the southwest quarter of the project area.

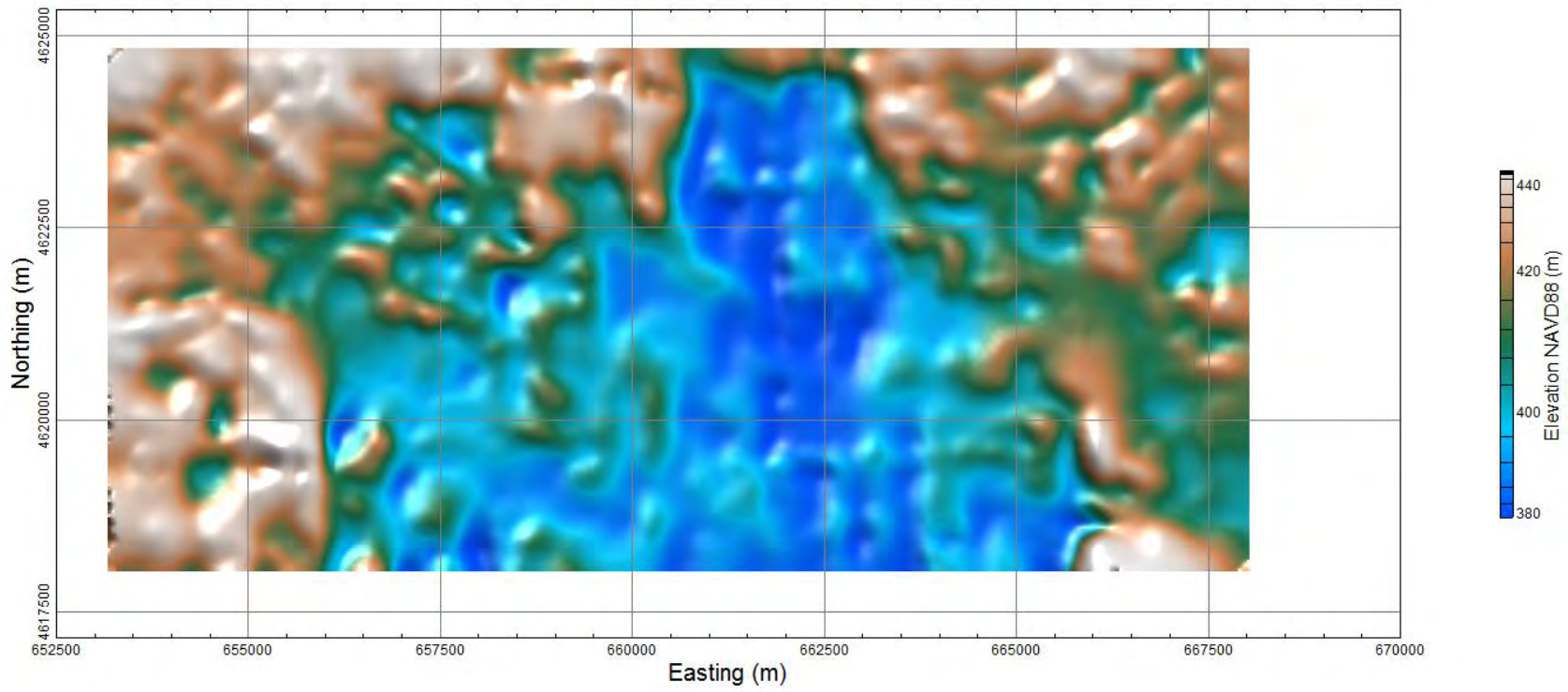


Figure A-3 – Cretaceous bedrock topography beneath Quaternary deposits.

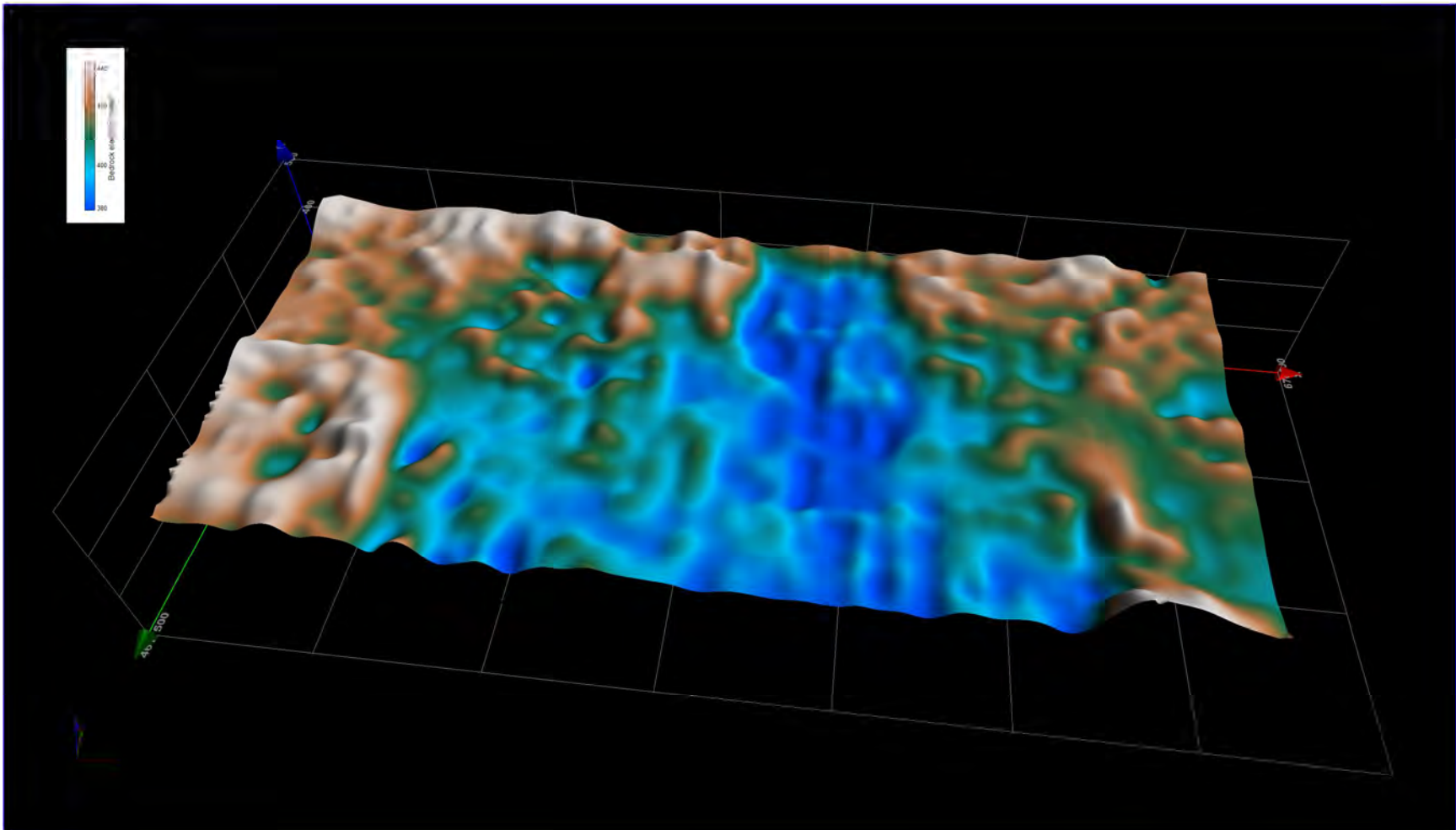


Figure A-4 – 3-D display of Cretaceous bedrock topography beneath Quaternary deposits.

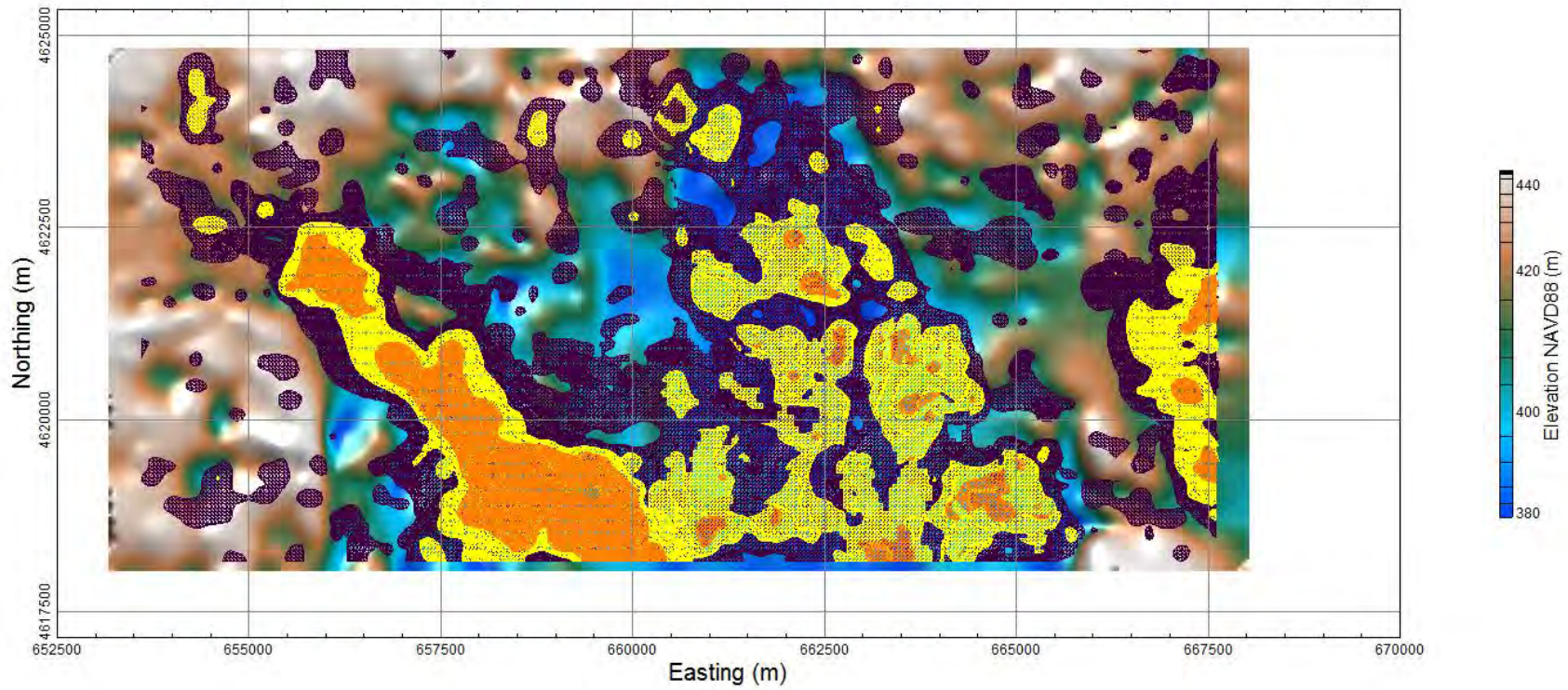


Figure A-5 – 15, 20, and 25 ohm-m resistivity surfaces overlying the Cretaceous bedrock surface.

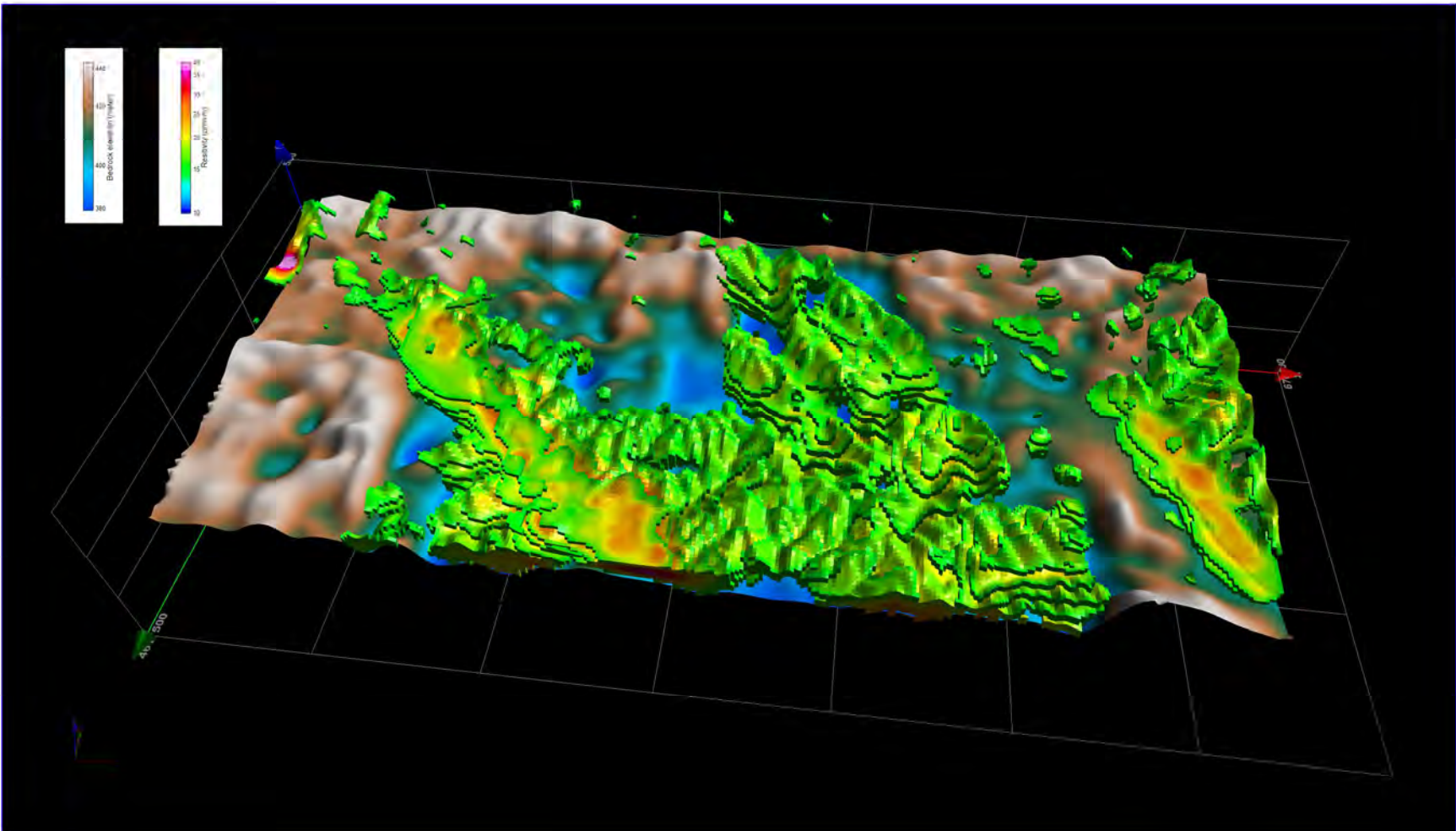


Figure A-6- 3-D voxel display of 15 ohm-m or greater resistivity zones overlying the Cretaceous bedrock surface.

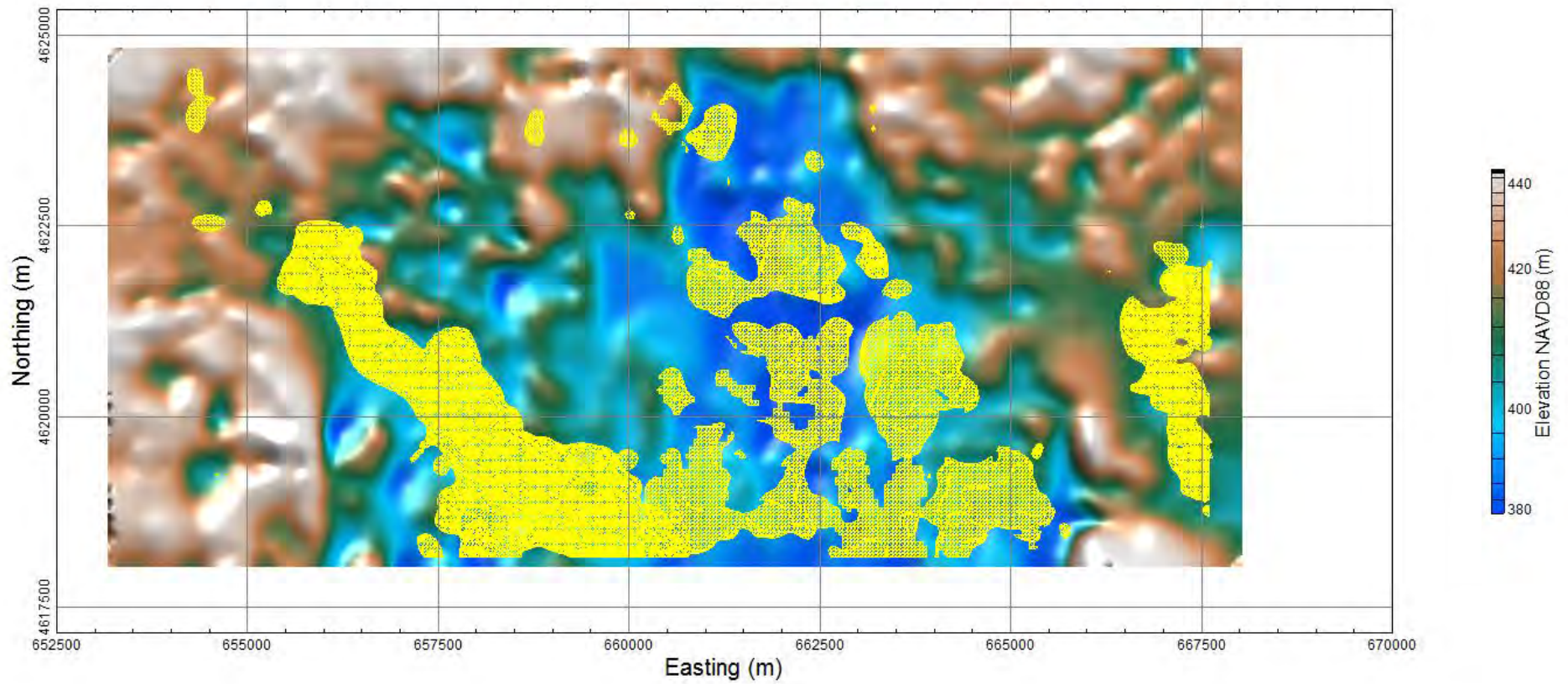


Figure A-7 – Areas of subsurface exhibiting resistivity at 20 ohm-m or greater overlying the Cretaceous bedrock surface.

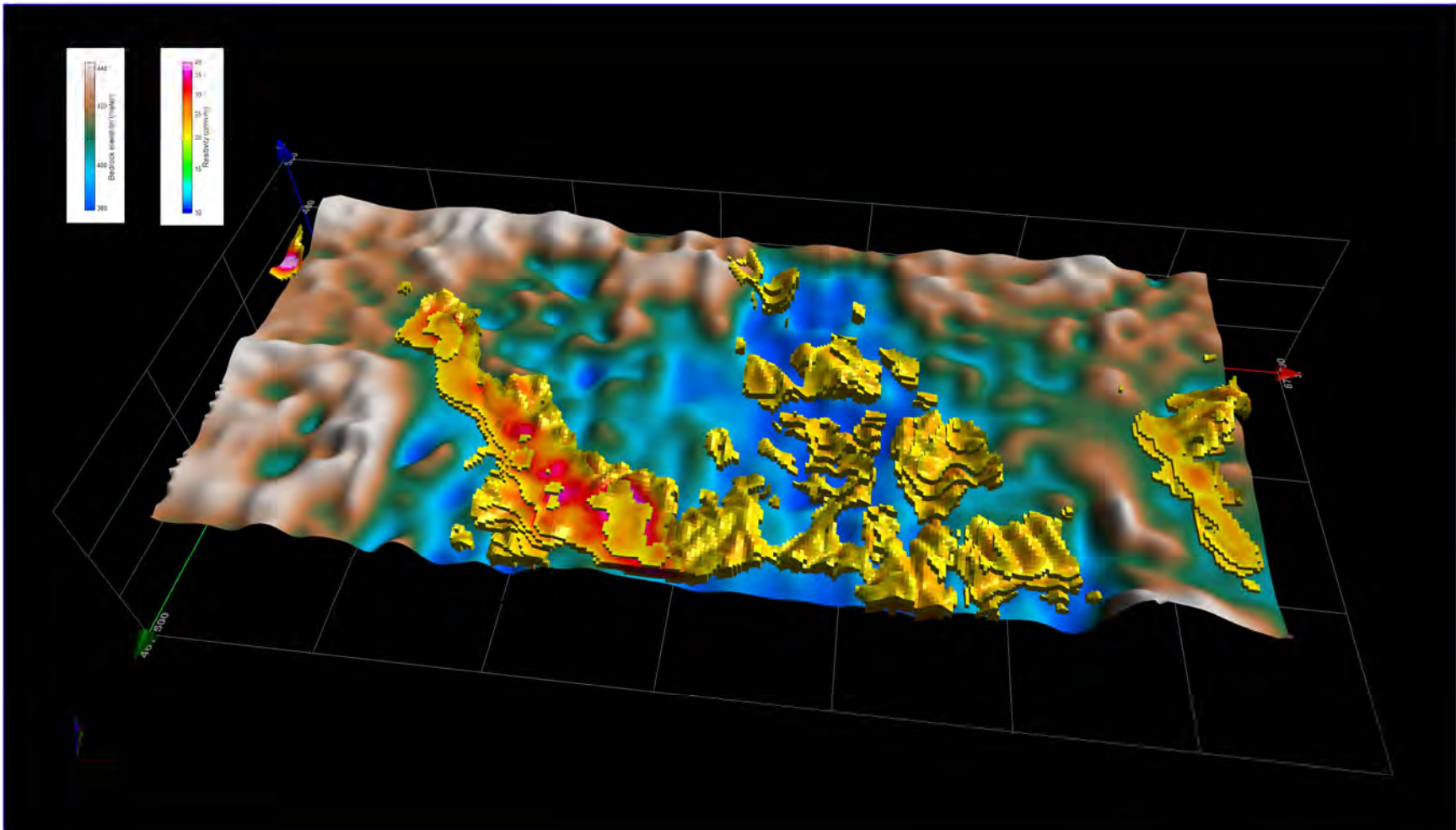


Figure A-8 – 3-D voxel display of 20 ohm-m or greater resistivity zones overlying the Cretaceous bedrock surface.

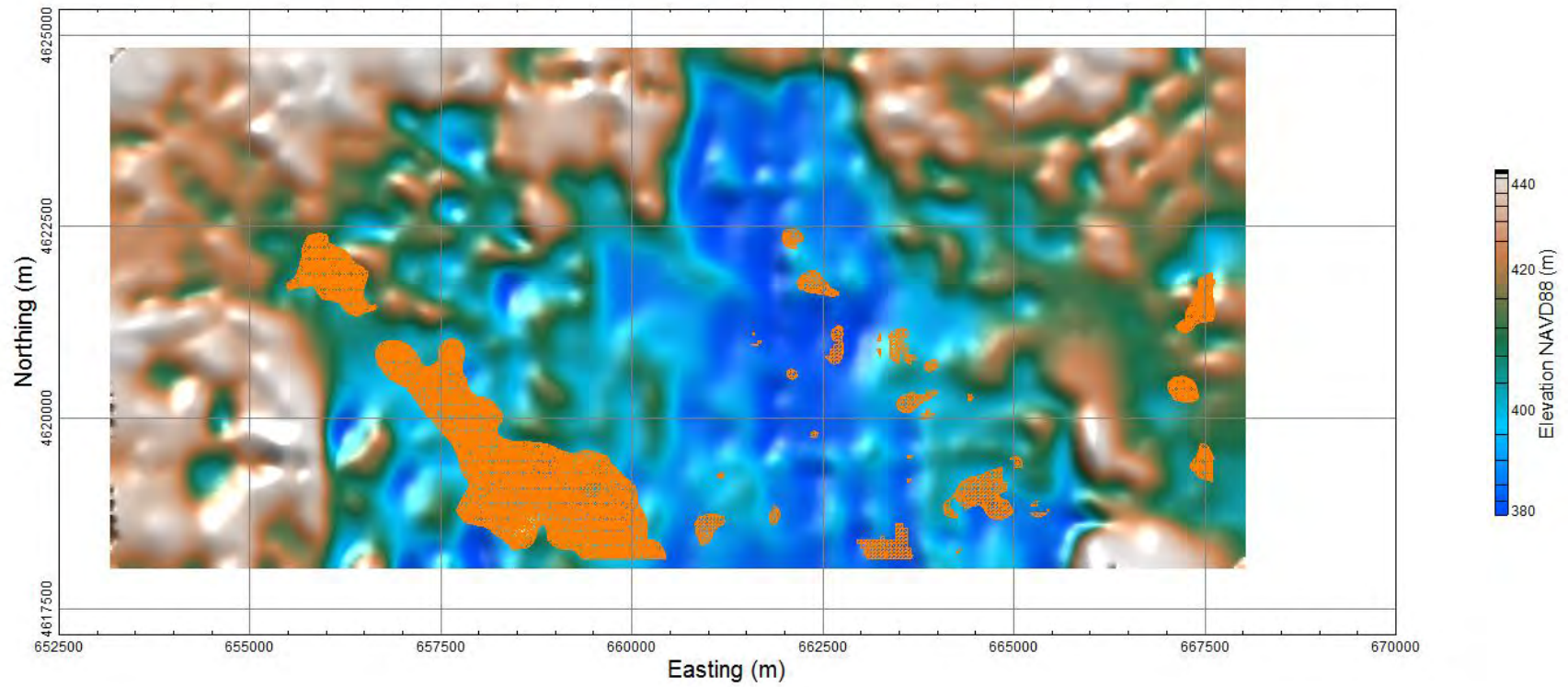


Figure A-9 – Areas of subsurface exhibiting resistivity at 25 ohm-m or greater overlying the Cretaceous bedrock surface.

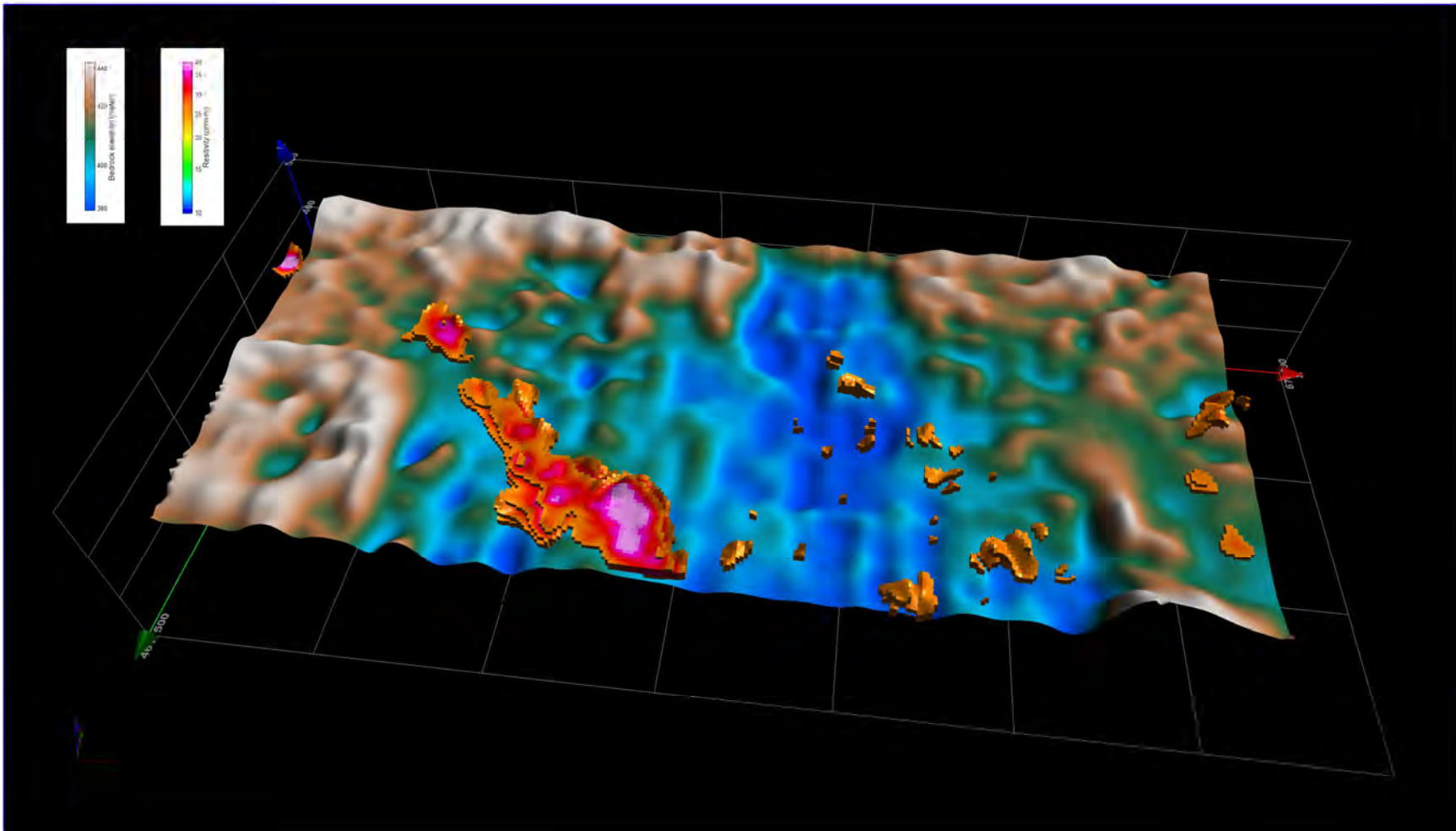


Figure A-10 – 3-D voxel display of 25 ohm-m or greater resistivity zones overlying the Cretaceous bedrock surface.

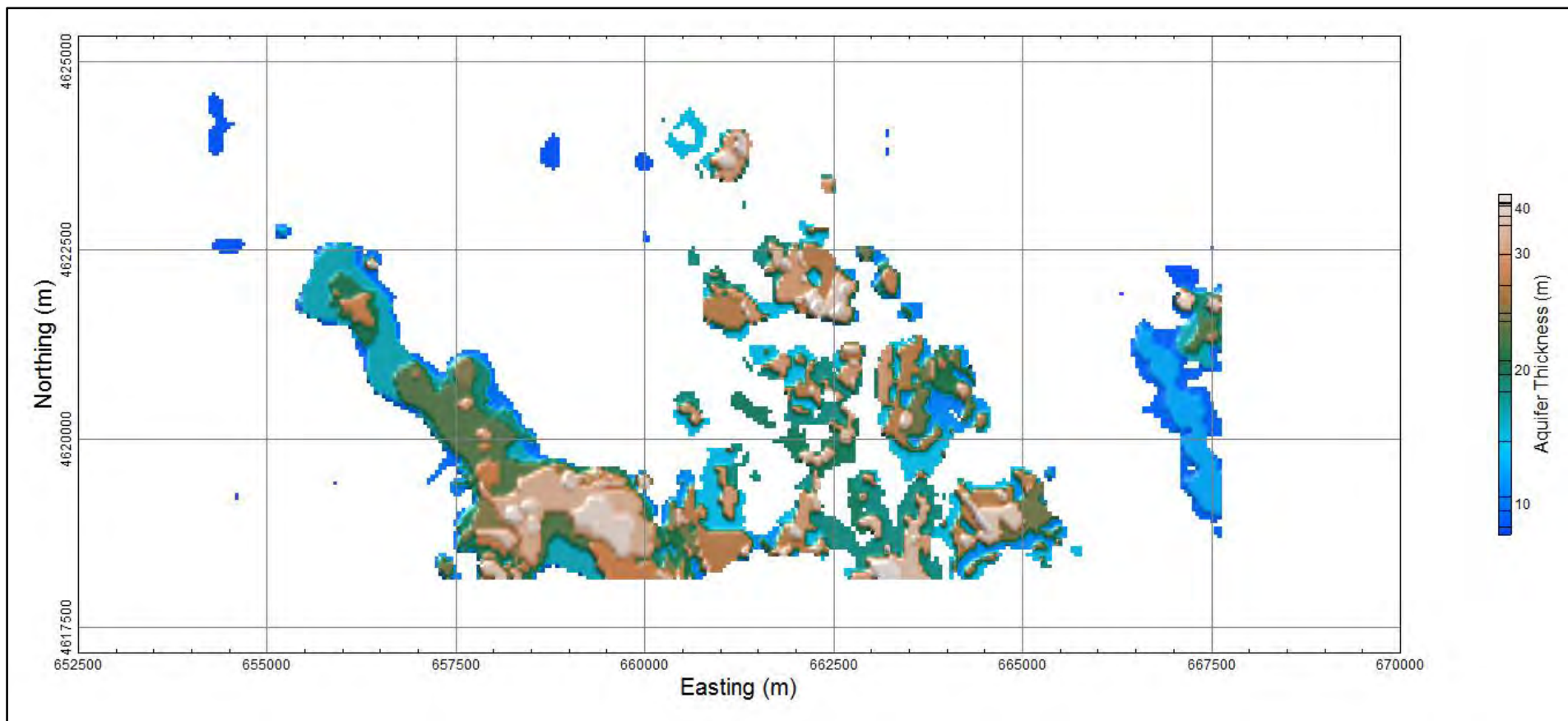


Figure A-11 – Thickness of principal aquifer area with resistivity levels at 25 ohm-m or greater.

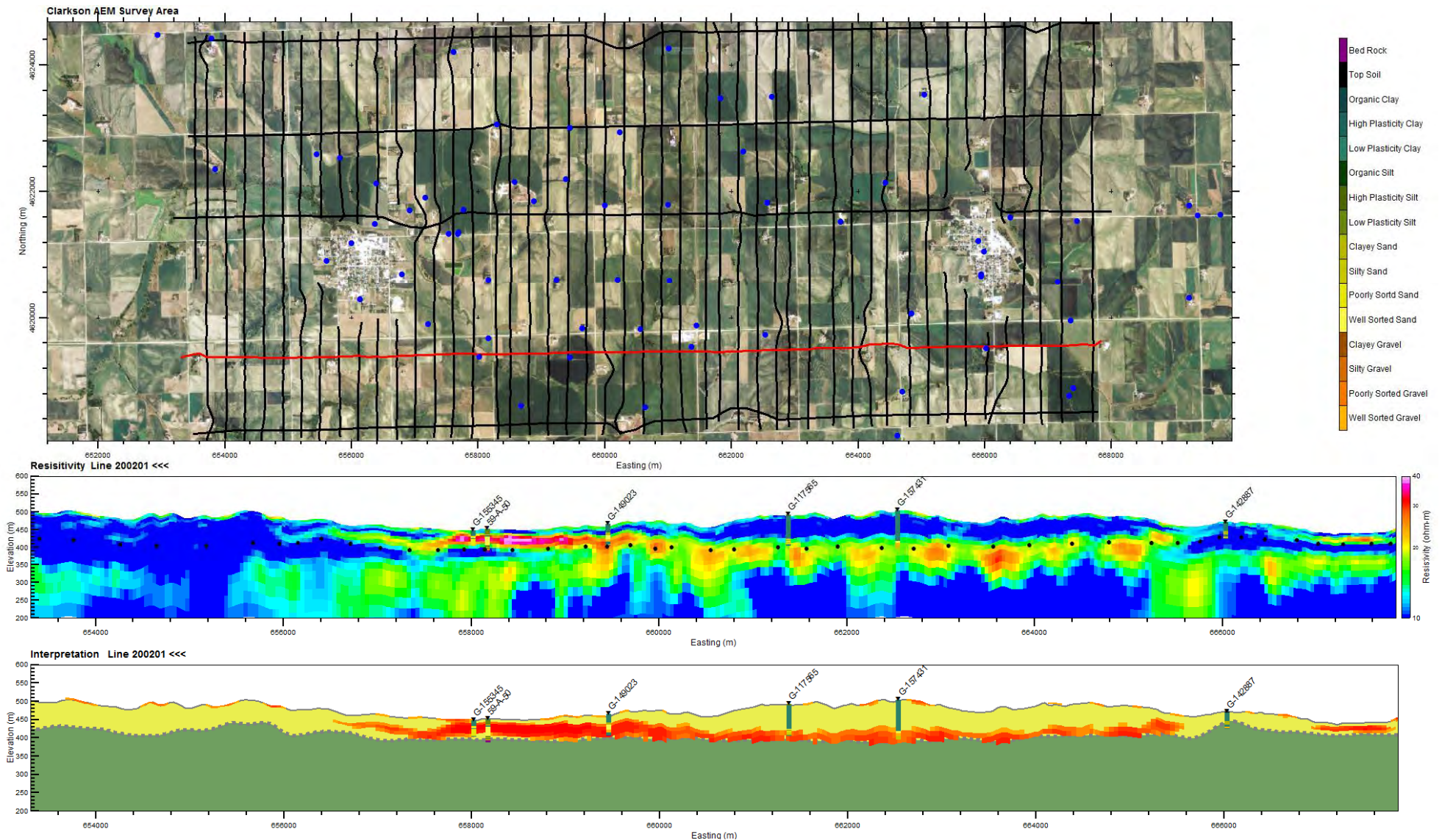


Figure A-12 – West to East cross section along the southern tie-line. AEM data collection locations (top map view), flight lines (black lines and red line is current viewed flight line), and borehole locations (blue dots); resistivity model (middle plot) with boreholes and interpreted top of the cretaceous bedrock (black dots); and the interpretation (bottom plot) of the cretaceous top of bedrock (green color), the Quaternary deposits (yellow color) and the extent of the principal aquifer (red color) (NAD83 UTM zone 17 N (meter), vertical datum is NAVD88 (meter)).

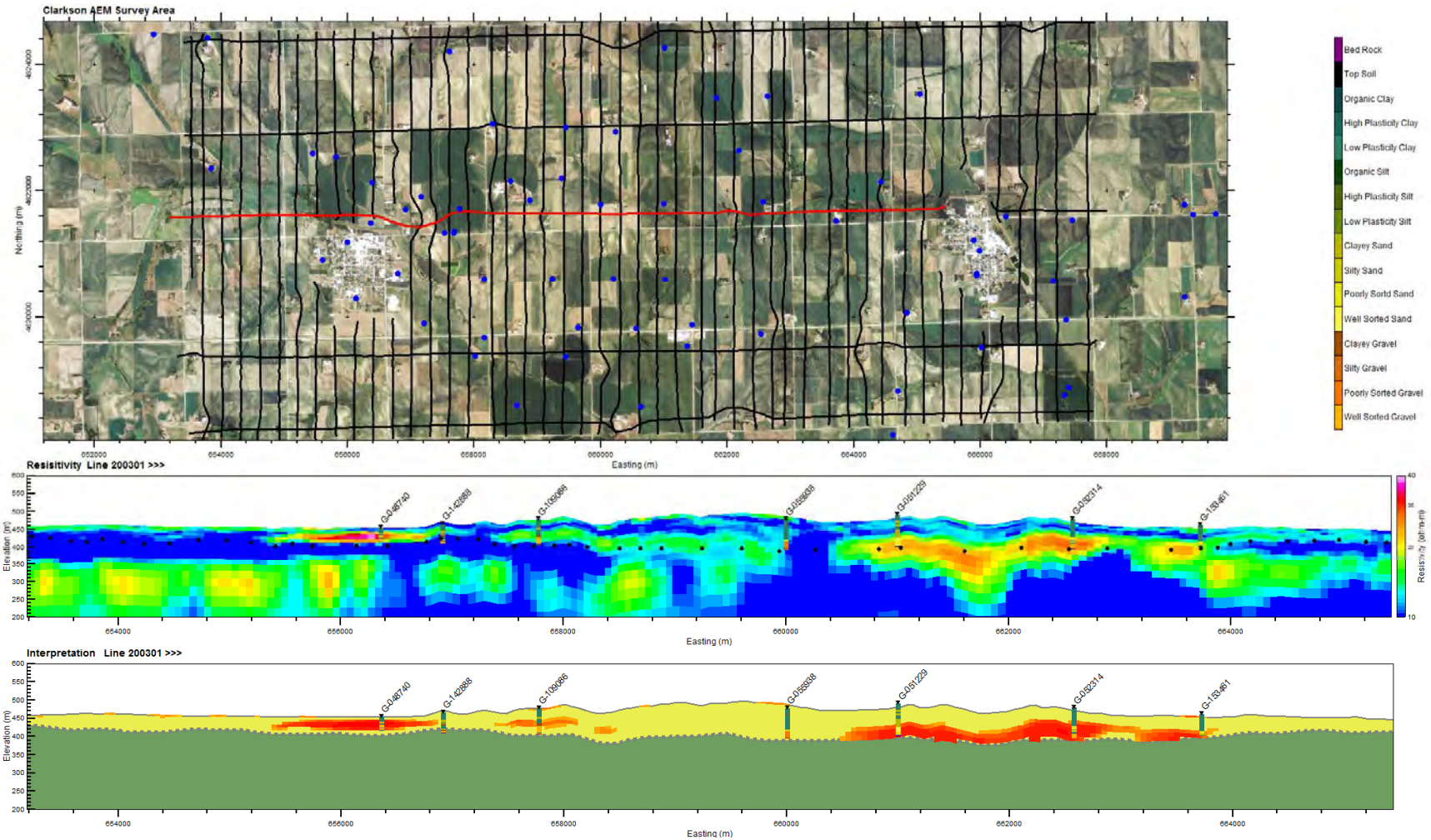


Figure A-13 – West to east cross section along the middle tie-line. AEM data collection locations (top map view), flight lines (black lines and red line is current viewed flight line), and borehole locations (blue dots); resistivity model (middle plot) with boreholes and interpreted top of the cretaceous bedrock (black dots); and the interpretation (bottom plot) of the cretaceous top of bedrock (green color), the Quaternary deposits (yellow color) and the extent of the principal aquifer (red color) (NAD83 UTM zone 17 N (meter), vertical datum is NAVD88 (meter)).

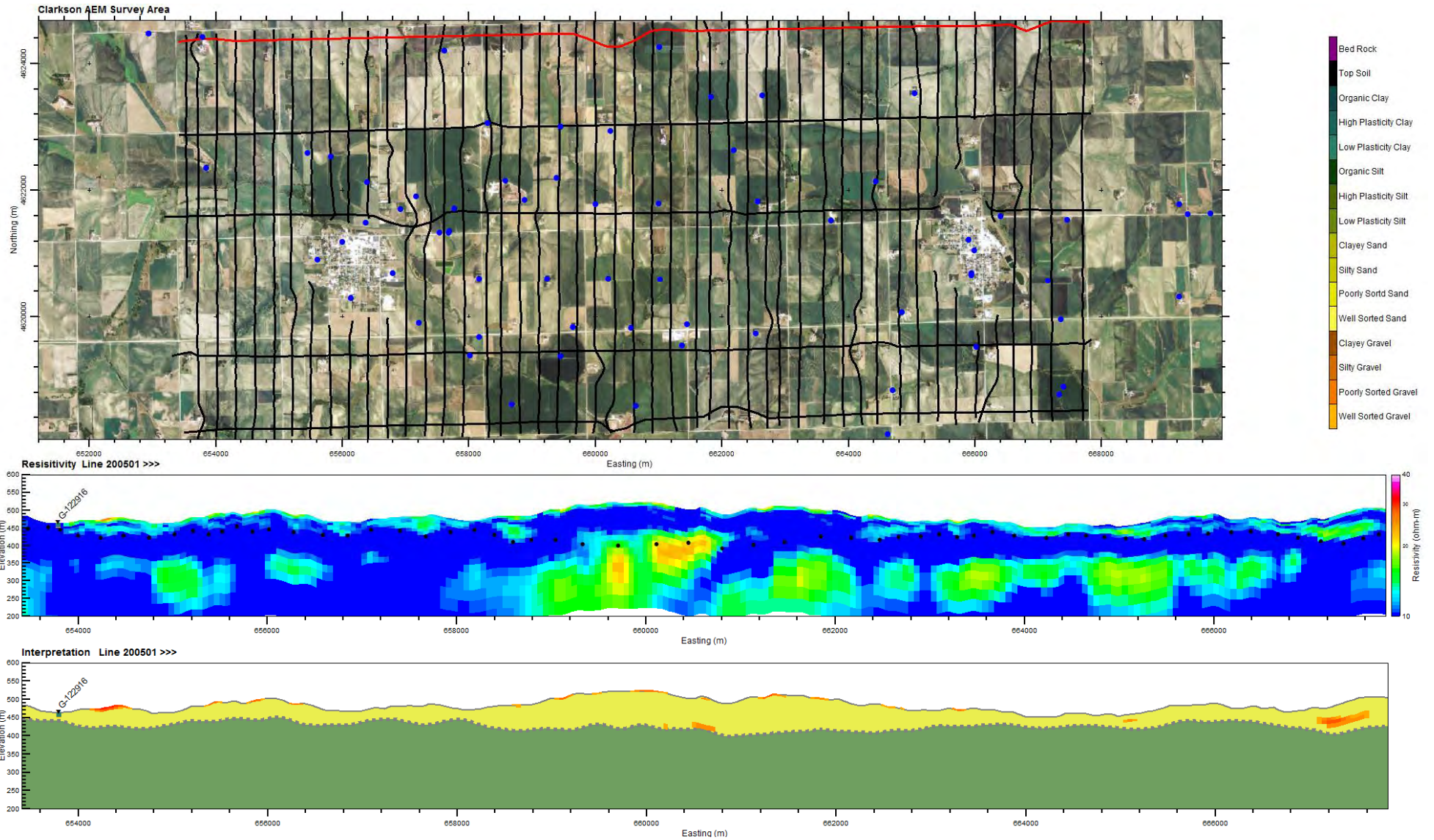


Figure A-14 – West to East cross section along the northern tie-line. AEM data collection locations (top map view), flight lines (black lines and red line is current viewed flight line), and borehole locations (blue dots); resistivity model (middle plot) with boreholes and interpreted top of the cretaceous bedrock (black dots); and the interpretation (bottom plot) of the cretaceous top of bedrock (green color), the Quaternary deposits (yellow color) and the extent of the principal aquifer (red color) (NAD83 UTM zone 17 N (meter), vertical datum is NAVD88 (meter)).

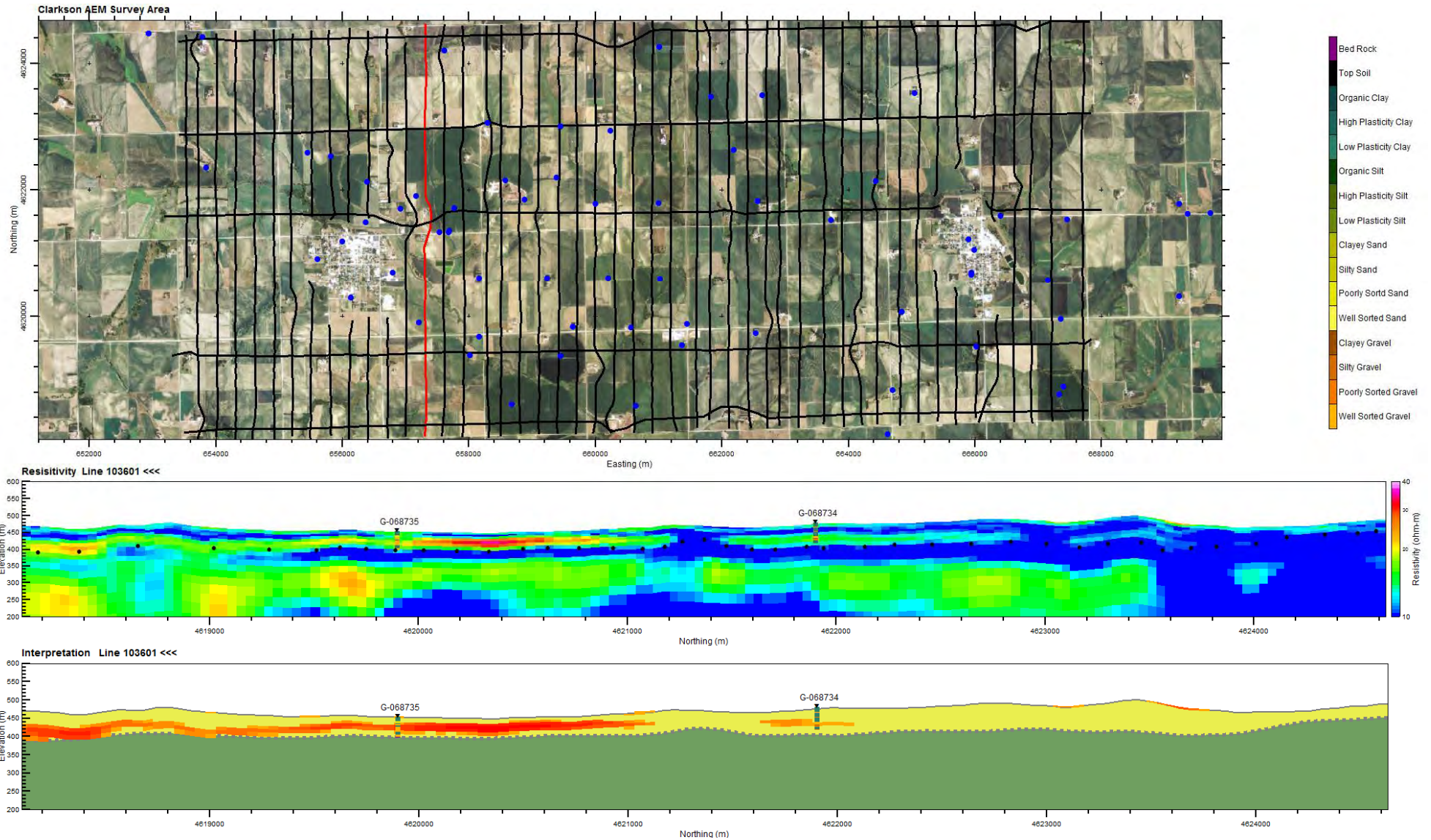


Figure A-15 – South to north cross section along a flight line east of Clarkson. AEM data collection locations (top map view), flight lines (black lines and red line is current viewed flight line), and borehole locations (blue dots); resistivity model (middle plot) with boreholes and interpreted top of the cretaceous bedrock (black dots); and the interpretation (bottom plot) of the cretaceous top of bedrock (green color), the Quaternary deposits (yellow color) and the extent of the principal aquifer (red color) (NAD83 UTM zone 17 N (meter), vertical datum is NAVD88 (meter)).

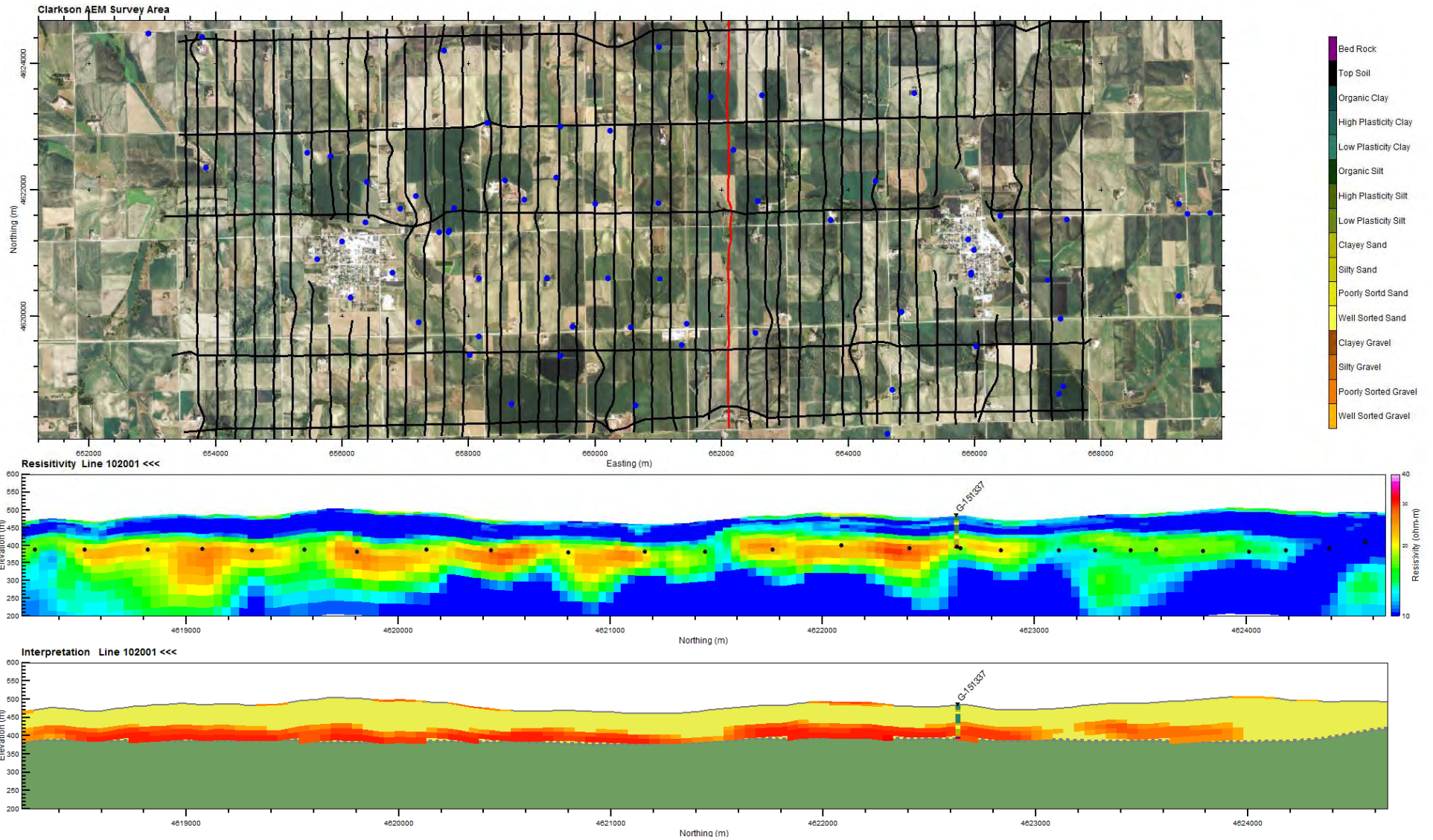


Figure A-16 – South to North cross section along a flight line east of Clarkson and west of Howells. AEM data collection locations (top map view), flight lines (black lines and red line is current viewed flight line), and borehole locations (blue dots); resistivity model (middle plot) with boreholes and interpreted top of the cretaceous bedrock (black dots); and the interpretation (bottom plot) of the cretaceous top of bedrock (green color), the Quaternary deposits (yellow color) and the extent of the principal aquifer (red color) (NAD83 UTM zone 17 N (meter), vertical datum is NAVD88 (meter)).

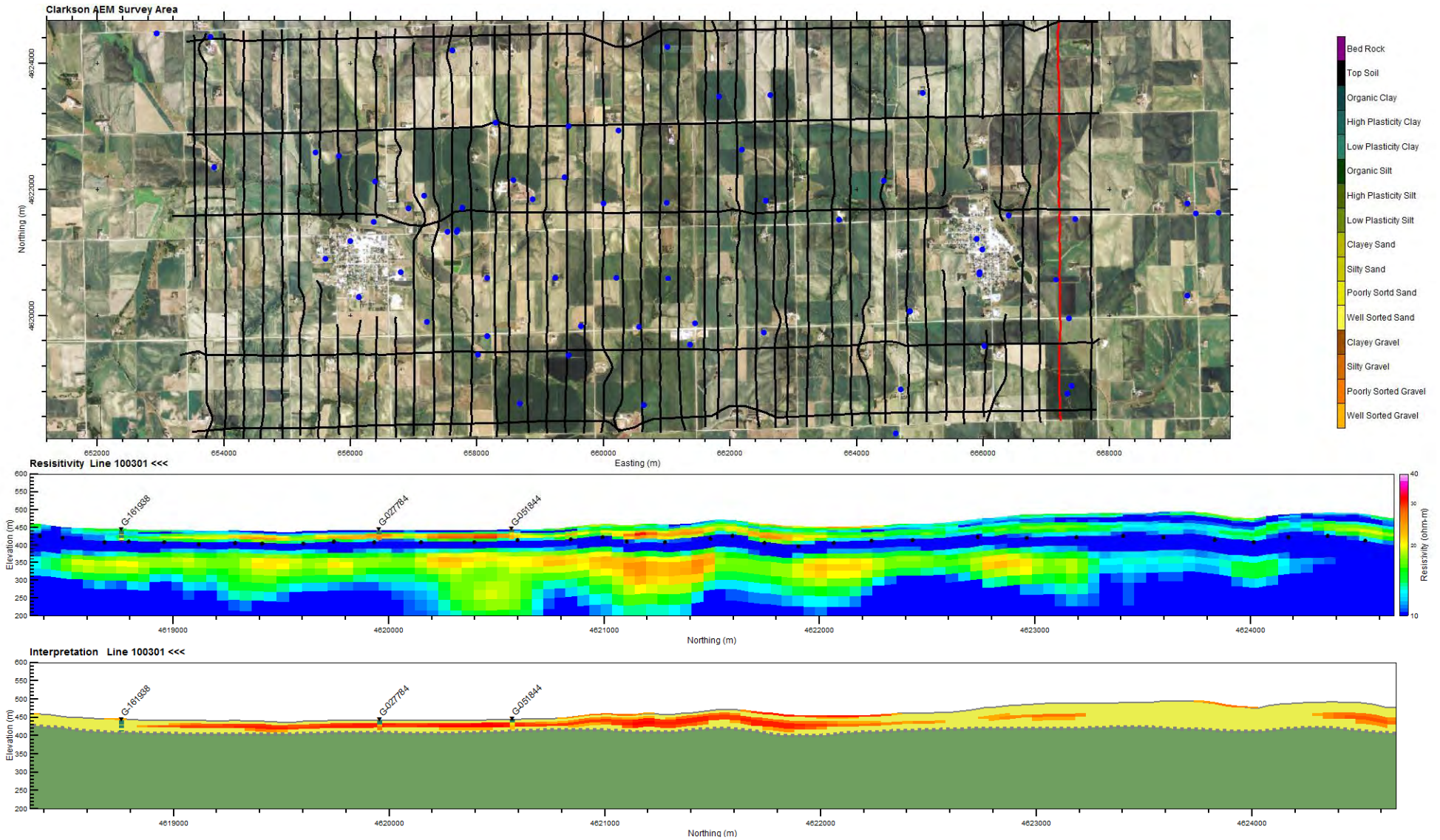


Figure A-17 – South to north cross section along a flight line west of Howells. AEM data collection locations (top map view), flight lines (black lines and red line is current viewed flight line), and borehole locations (blue dots); resistivity model (middle plot) with boreholes and interpreted top of the cretaceous bedrock (black dots); and the interpretation (bottom plot) of the cretaceous top of bedrock (green color), the Quaternary deposits (yellow color) and the extent of the principal aquifer (red color) (NAD83 UTM zone 17 N (meter), vertical datum is NAVD88 (meter)).

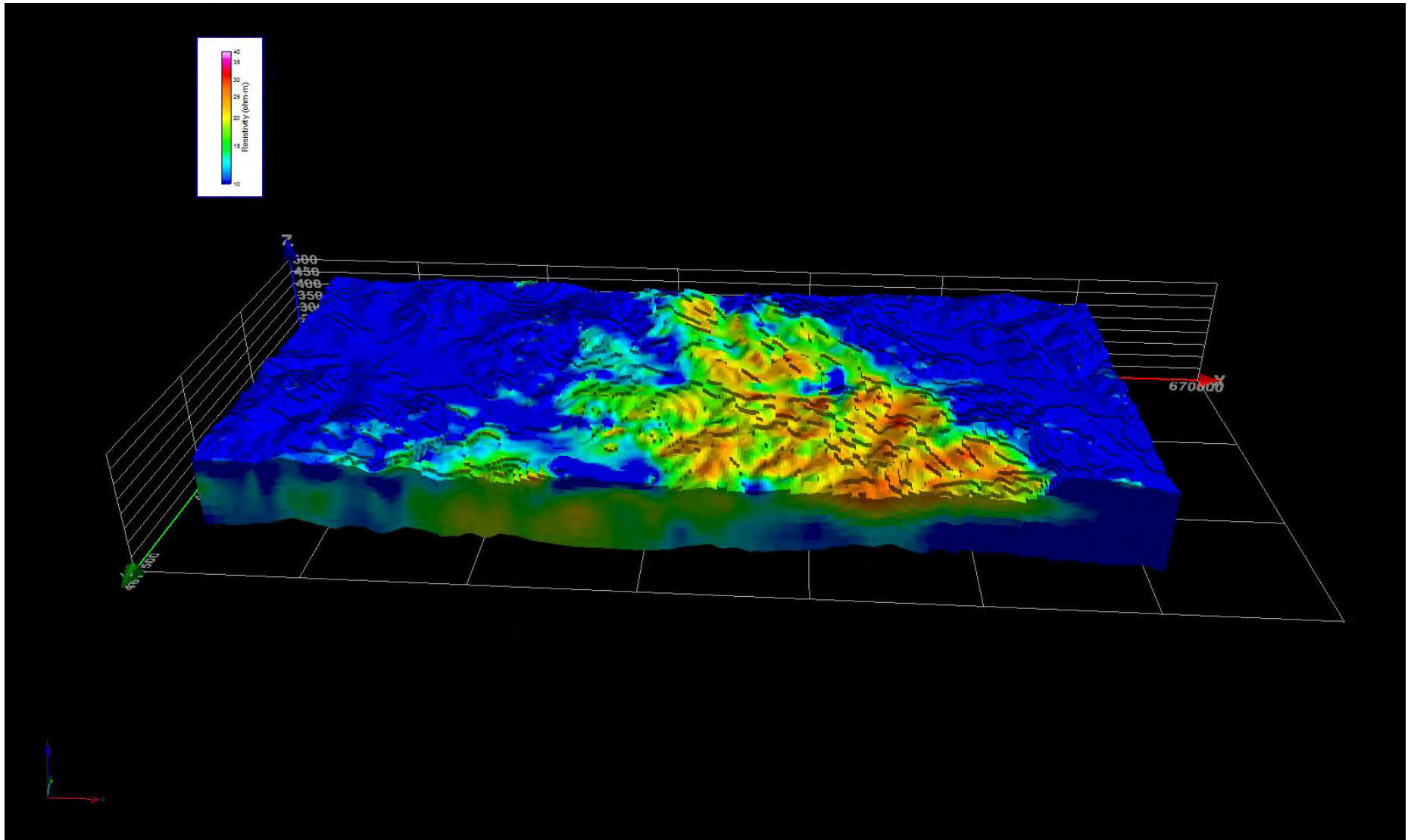


Figure A-18 – Resistivity of the Cretaceous bedrock units beneath the Quaternary system and principal aquifer.

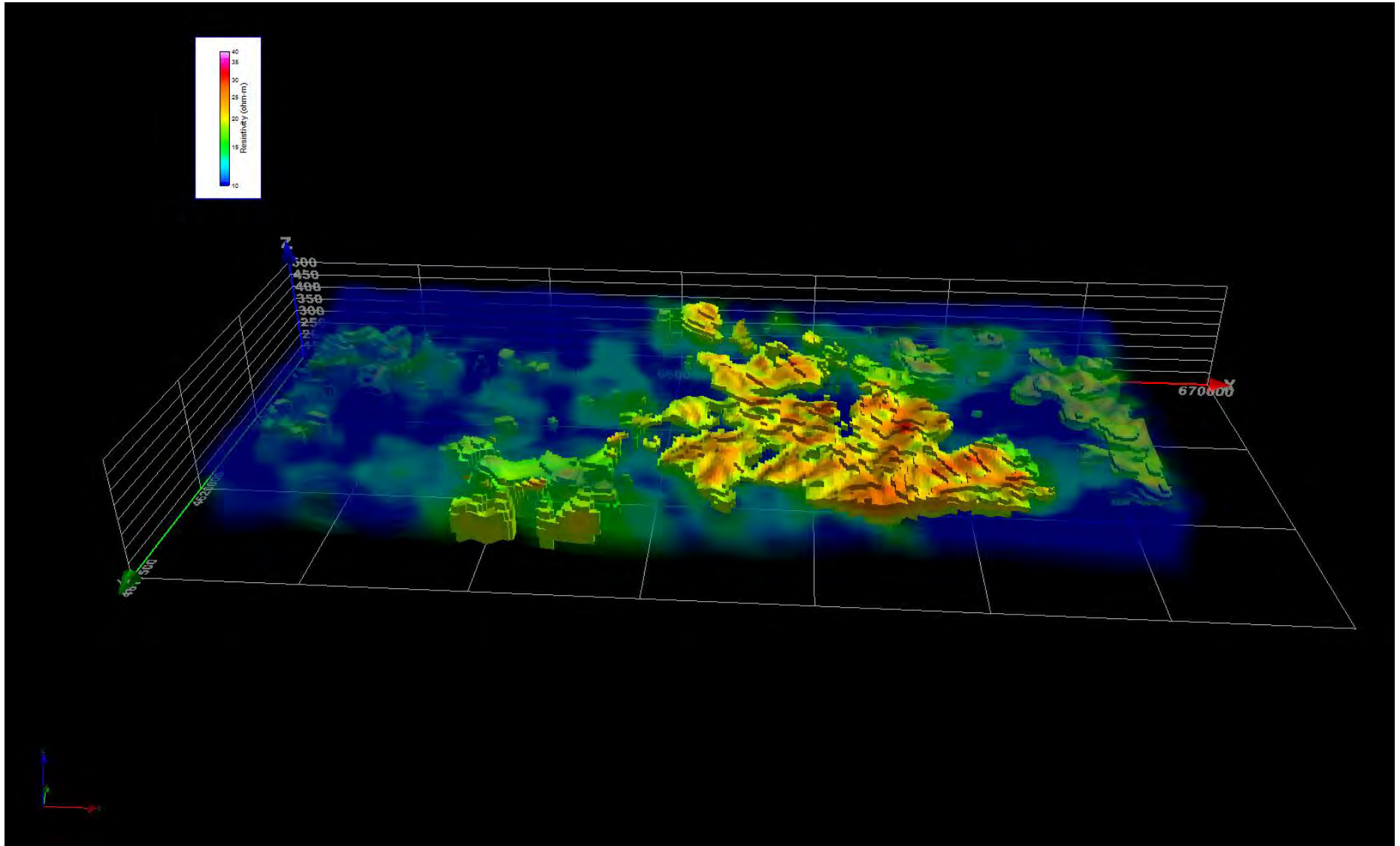


Figure A-19 – 3-D cloud display image of 18 ohm-m voxel in the Cretaceous bedrock underlying the Quaternary System and principal aquifer.

Appendix 2- Metadata

Metadata File Formats

The acquired and processed data are provided in the form of .XYZ files. The included files are:

- Clarkson_Inversion.xyz: results of inversion of AEM data, given in an array of modeled layers and earth resistivity
- Clarkson_AEM_MAG_data.xyz: results if AEM survey giving raw and processed magnetic and electromagnetic data

The data in these file are separated according to planned flight lines. The projection of the spatial data in the .XYZ files are given in UTM Zone 14N easting and northing (NAD83). The parameters within the both of the .XYZ files are listed in Tables A-1 and A-2.

Table A-1 - Parameters for metadata file Clarkson_Inversion.xyz

Parameter	Description	Unit
X	Easting NAD83 UTM Zone 14 North	Meter [m]
Y	Northing NAD83 UTM Zone 14 North	Meter [m]
TOPO	Helicopter recorded topography NAVD88	Meter [m]
ALT	Altitude recorded of SkyTEM sensor	Meter [m]
INVALT	Inverted Altitude	Meter [m]
DELTAALT	Difference from recorded and inverted altitude	Meter [m]
DEM_sample	The sampling of the USGS NED DEM	Meter [m]
RES[xx*]	Inverted layer resistivity value	Ohm-meter [$\hat{\delta}$ m]
RES_STD[xx*]	Standard deviation of resistivity for inverted layer	Ohm-meter [$\hat{\delta}$ m]
SIGNA[xx*]	Model versus data misfits for layer	N/A
TOP[xx*]	Inverted layer top	Meter [m]
Bottom[xx*]	Inverted layer bottom	Meter [m]
THK[xx*]	Inverted layer thickness	Meter [m]
DEP_BOT_STD[xx*]	Inverted layer standard deviations	N/A
DOI_UPPER	A numerical upper estimate of the depth of investigation	Meter [m]
DOI_Lower	A numerical lower estimate of the depth of investigation	Meter [m]
CHORDLEN	Distance between points	Meter [m]

*There are a total of 18 inverted layers, numbered 0-17.

Table A-2- Parameters for metadata file Clarkson_AEM_MAG_data.xyz

Parameter	Description	Unit
Alt	DGPS Altitude	Meters above sea level
AngleX	Angle (in flight direction)	Degrees
AngleY	Angle (perpendicular to flight direction)	Degrees
Bmag_Diur	Diurnal Variation - magnetic base station data	nanotesla [nT]
Bmag_raw	Total Magnetic Intensity . raw magnetic data . magnetic base station data	nanotesla [nT]
Curr_1	Current, High Moment	Amps
Curr_2	Current, Low Moment	Amps
Date	Date	yyyymmdd
DateTime	DateTime Format	Decimal days
DEM	Digital Elevation Model	Meters above sea level
E_NAD83	UTM Zone 14N (NAD83)	Meter [m]
Fid	Unique Fiducial Number	Seconds
Flight	Name of Flight	yyyymmdd.ff
GdSpeed	Ground Speed	Kilometers/hour [km/h]
Height	Filtered Height Measurement	Meters [m]
HM_X_G15[xx*]	Normalized High Moment X-RxCoil value	$\mu V/(m^4 \cdot A)$
HM_Z_G15[xx*]	Normalized High Moment Z-RxCoil value	$\mu V/(m^4 \cdot A)$
IGR_TMI	Calculated IGRF-10	nanotesla [nT]
Lat	Latitude, WGS84	Decimal Degrees
Line	Line Number	LLLLLL
LM_X_G10[xx*]	Normalized Low Moment X-RxCoil value	$\mu V/(m^4 \cdot A)$
LM_Z_G10[xx*]	Normalized Low Moment Z-RxCoil value	$\mu V/(m^4 \cdot A)$
Lon	Longitude, WGS84	Decimal Degrees
Mag_cor	Residual Magnetic Field . corrected for diurnal, lag, heading and IGRF	nanotesla [nT]
Mag_fil	Filtered Magnetic Data	nanotesla [nT]
Mag_raw	Raw Magnetic Data . total magnetic intensity - despiked	nanotesla [nT]
N_NAD83	UTM Zone 14N (NAD83)	Meter
PLNI_60Hz	Power Line Noise Intensity. Amplitude spectral density of the power line noise	N/A
RMF	Residual Magnetic Field . IGRF removed . final corrected and leveled magnetic data	nanotesla [nT]
Time	Time	hhmmss.sss
TMI	Total Magnetic Intensity . final corrected and leveled magnetic data; IGRF recalculated	nanotesla [nT]

*High Moment and low moment measurement channels correspond with time gate numbers listed in Table A-3.

All recorded data are time stamped in order to correlate independent data sets. The time stamps are in Coordinated Universal Time/Greenwich Mean Time (UTC/GMT) which is a +6 hour difference from Central Standard Time. Time stamps are one of the two following formats.

- Date and time defined as: yyyy/mm/dd hh:mm:ss.sss
- Date and time values defined as the number of days since 1900/01/01 and seconds of the day: dddd.ssssssss (decimal days).

Time Gates

There are a total of 38 time gates, Table A-3 presents the gate number, the gate center, gate width and a comment concerning time gate usage.

Table A-3 - Time Gate Information

Gate No.	Gate Center (μs)	Gate Width (μs)	Comment	Gate No.	Gate Center (μs)	Gate Width (μs)	Comment
0	-0.385	1.57	Not Used	19	172.115	38.57	Low and High Moment
1	1.615	1.57	Not Used	20	216.115	48.57	Low and High Moment
2	3.615	1.57	Not Used	21	271.615	61.57	Low and High Moment
3	5.615	1.57	Not Used	22	342.115	78.57	Low and High Moment
4	7.615	1.57	Not Used	23	431.615	99.57	Low and High Moment
5	9.615	1.57	Low Moment Only	24	544.615	125.57	Low and High Moment
6	11.615	1.57	Low Moment Only	25	687.115	158.57	Low and High Moment
7	13.615	1.57	Low Moment Only	26	867.115	200.57	Low and High Moment
8	16.115	2.57	Low Moment Only	27	1094.615	253.57	Low and High Moment
9	19.615	3.57	Low Moment Only	28	1382.115	320.57	Low and High Moment
10	24.115	4.57	Low Moment Only	29	1745.115	404.57	High Moment Only
11	29.615	5.57	Low Moment Only	30	2203.115	510.57	High Moment Only
12	36.615	5.57	Low Moment Only	31	2781.615	645.57	High Moment Only
13	45.615	9.57	Low Moment Only	32	3512.615	815.57	High Moment Only
14	56.615	11.57	Low and High Moment	33	4436.115	1030.57	High Moment Only
15	70.115	14.57	Low and High Moment	34	5602.615	1301.57	High Moment Only
16	87.115	18.57	Low and High Moment	35	7075.615	1643.57	High Moment Only
17	109.115	24.57	Low and High Moment	36	8936.115	2076.57	High Moment Only
18	137.115	30.57	Low and High Moment	37	11286.115	2622.57	High Moment Only

Appendix 3- Ancillary Data

Appendix 3- Ancillary Data

Instrumentation

Instrumentation of the SkyTEM includes a time domain electromagnetic (TDEM) system (one transmitter [Tx] and two receivers [Rx] positioned orthogonally in line with the x and z axes) and a magnetometer as well as data acquisition systems for both of these instruments. The SkyTEM also includes two each of laser altimeters, inclinometers/tilt meters and DGPS receivers. Positional data from the frame mounted DGPS receivers are recorded by the TDEM data acquisition system. The magnetometer includes a third DGPS receiver, this positional data is recorded by the magnetometer data acquisition system. Figure A-20 gives a simple illustration of the SkyTEM frame and instrument locations, the image is viewed along the +z axis looking at the horizontal x-y plane. The axes for the image are labelled with distance in meters. The square symbols denote the locations of the altimeters, the triangles denote the DGPS positions and the circles denote the inclinometers. The magnetometer is located on a boom off the front of the frame (right side of image, arrow indicates +x direction as well as direction of flight). The TDEM Tx coil is located around the octagonal frame and the Rx Coils (x and z) are located at the back of the frame, left side of image).

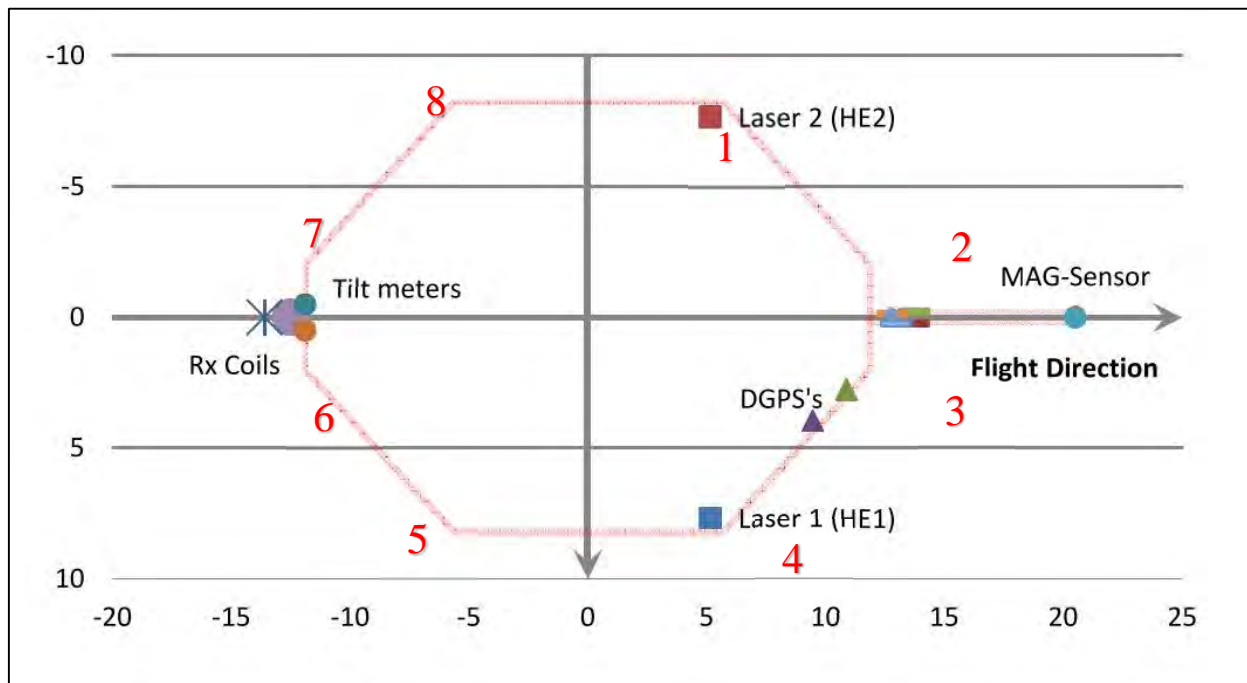


Figure A-20 - Simple illustration of SkyTEM frame including instrument locations.

The coordinate system used defines the +x direction as the direction of flight, the +y direction is defined 90° to the right and the +z direction is downward. The center of the transmitter loop, mounted to the octagonal SkyTEM frame is used as the origin when considering instrumentation positions. The Table A-4 lists the positions of the instruments (in meters) and Table A-5 lists the corners of the transmitter loop (labeled in red numbers in Figure A-20).

Table A-4 - Instrumentation positions on SkyTEM frame.

Instrument	DGPS 1	DGPS 2	Inclinometer 1	Inclinometer 2	Altimeter HE1	Altimeter HE2	X Rx Coil	Z Rx Coil
X	9.90	9.90	-11.65	-11.65	5.13	5.13	-13.60	-12.50
Y	2.69	3.66	0.50	0.50	7.85	-7.79	0.00	0.00
Z	-0.28	-0.28	-0.37	-0.37	-0.13	-0.13	-0.02	-2.21

Table A-5 - Corner positions of Tx loop on SkyTEM frame.

TX Corners	1	2	3	4	5	6	7	8
X	5.68	11.87	11.87	5.68	-5.68	-11.87	-11.87	-5.68
Y	8.22	2.03	-2.03	-8.22	-8.22	-2.03	2.03	8.22

DGPS and magnetometer base stations were placed at the locations listed in Table A-6. The geodetic reference used is NAD83; the unit of measurement is in meters.

Table A-6 - Locations of base station instruments.

Instrument	UTM X, easting	UTM Y, northing	UTM Zone	Elevation
DGPS Base Station	645119	4618553	14N	467.03
Magnetometer Base Station	644406	4619213	14N	505